

# **STEADY THREE-DIMENSIONAL SHOCK WAVE REFLECTION TRANSITION PHENOMENA**

**Jeffrey Baloyi**

A research report submitted to the Faculty of Engineering and the Built Environment, of the University of the Witwatersrand, in partial fulfilment of the requirements for the degree of Master of Science in Engineering.

Johannesburg 2008

## Formal declaration

I declare that this research report is my own unaided work. It is being submitted for the Degree of Master of Science in Engineering to the University of the Witwatersrand. I also declare that all references or sources cited in this research report were properly acknowledged. I also declare that the work undertaken for this research report was done while I was under the employ of the Council for Scientific and Industrial Research (CSIR).

.....  
Jeffrey Baloyi

..... day of ..... year .....  
*Day month year*

## Abstract

Shockwave reflection has in recent times been investigated as a three-dimensional phenomenon where geometrical effects on the reflection patterns have been given more attention than previously. A typical example is that of a supersonic body flying over a ground plane, in which the bow wave reflects off the ground surface. Depending on the Mach number, the reflection can be regular below the body, but will then make a transition to the three-shock Mach reflection pattern at some lateral position. In this report symmetrically arranged wedges with a finite span (i.e. one above the other) were modeled and visualised in CFD in order to investigate the three-dimensional steady state transition from regular reflection to Mach reflection. This follows on the work done by Skews (2000) where it was observed from shadowgraph pictures that there seems to be a sudden jump at the transition point in the growth of the Mach stem.

Contrary to what was observed by Skews (2000), the transition was found to be gradual and smooth in the current CFD simulations. High visual clarity from the CFD results could not be achieved, even after successive grid refinements were performed on and around the shockwaves, because of the averaging technique of fluid property values in cells performed by CFD codes. The flows in the vicinity of the transition are examined, with particular attention to the shear layers that are generated from the triple point lines. Because of the inclination of the Mach stem surface to the oncoming flow the Mach number behind this surface can be supersonic, in contrast to the two-dimensional case.

The steady state reflection phenomenon where there is transition from Mach reflection to regular and then back to Mach reflection when moving laterally outward from the vertical symmetry plane was also investigated using the same CFD setup, but with a much wider wedge span. This particularly interesting situation suggests the existence of complex transition criteria. The

aim was to reproduce numerically this phenomenon observed experimentally by Ivanov et al. (1999), and to see if these results can be replicated for a lower Mach number attainable using a local wind tunnel. Both aims were achieved, but with the same limitation mentioned above of the averaging technique of fluid property values by CFD codes. There are currently no analytical criteria for the prediction of shock wave reflection transition in the three-dimensional case, nor for the possible existence of a dual solution domain, as exist for two-dimensional flows. Parametric studies of the type discussed in this report should lead to a fuller understanding of the flow conditions of importance.

## **Acknowledgements**

I firstly would like to thank my supervisor, Prof. B W Skews, for his guidance and support throughout the time I had been registered as a student. Secondly I would also like to thank the National Research Foundation (NRF) for the funding granted to me through my supervisor. Last and not least I would also like to thank the Council for Scientific and Industrial Research (CSIR) for making time available for me to be able to do my research work while being employed by them, and also making their computer resources available for use for my research.

## Table of contents

Formal declaration .....	i
Abstract.....	ii
Acknowledgements.....	iv
Table of contents .....	v
List of figures.....	vi
Nomenclature.....	x
Introduction .....	1
Background and literature review.....	8
Objectives .....	13
Method and procedure.....	14
Case descriptions.....	14
Single transition Case.....	15
Double transition case .....	16
Discussion of results .....	19
Double transition Case .....	19
Single transition case .....	32
Conclusions .....	48
References.....	49
Appendix A: Additional pictures for the double transition case.....	51
Appendix B: Additional pictures for the single transition case.....	53
Appendix C: Detailed dimensions of the wedge setup for each test case.....	55

## List of figures

Figure 1: Regular reflection in steady state flow. Physical (left) and shock polar (right). Adapted from Hornung (1986).....	2
Figure 2: Mach reflection in steady state flow. Physical (left) and shock polar (right). Adapted from Hornung (1986).....	2
Figure 3: A shock polar diagram showing the condition at which the shock wave angle is the von Neumann angle. ....	4
Figure 4: A shock polar diagram showing the condition at which the shock wave angle is the detachment angle (solid line) or the sonic angle (dashed line). ....	5
Figure 5: The von Neumann and detachment criteria as functions of Mach number for a specific-heat ratio of 1.4, where $\alpha_d$ is the detachment criterion angle, $\alpha_N$ is the von Neumann criterion angle and $\alpha$ is the incident shock wave angle. ....	7
Figure 6: An oblique shadowgraph picture showing transition from regular reflection to Mach reflection, taken by Skews (2000).....	8
Figure 7: Conventional shadowgraph showing regular reflection. Adapted from Brown and Skews (2004).....	9
Figure 8: Orthogonal shadowgraph corresponding to figure 7. Adapted from Brown and Skews (2004).....	9
Figure 9: Laser sheet images at different span-wise positions ( z ) taken by Ivanov et al. (1999). ....	10
Figure 11: shadowgraph pictures showing the absence of influence on the Mach stem height by downstream flow conditions. Adapted from Chpoun and Leclerc (1999).....	12
Figure 12: Pictures showing arrangements of the two wedges used in the Single transition case.....	16
Figure 13: Pictures showing arrangements of the two wedges used in the Double transition case. ....	17
Figure 14: CFD pictures at span-wise positions ( z ) of, from left to right 0 mm, 158 mm and 198 mm, obtained using Fluent for $M_\infty = 4.0$ .....	21
Figure 14: Laser sheet Images at different span-wise positions ( z ) taken by Ivanov et al. (1999) for $M_\infty = 4.0$ . ....	21

Figure 16: CFD pictures at span-wise positions (z) of, from top to bottom 0 mm, 158 mm and 198 mm, obtained using Fluent for $M_\infty = 3.1$ .....	22
Figure 17: CFD pictures at span-wise positions (z) of, from top to bottom 0 mm, 158 mm and 198 mm, obtained using Fluent for $M_\infty = 2.9$ .....	23
Figure 18: A flooded plan view of Mach number plotted on the horizontal symmetry plane. This is for $M_\infty = 3.1$ . ....	24
Figure 19: A flooded plan view of pressure plotted on the horizontal symmetry plane. This is for $M_\infty = 3.1$ .....	25
Figure 20: A plan view plot of a slip surface (shear layer) with streamlines moving from right to left plotted on the horizontal symmetry plane, with the wedge in the background. This is for $M_\infty = 3.1$ .....	26
Figure 21: A plan view plot of entropy on the horizontal symmetry plane. This is for $M_\infty = 3.1$ . ....	27
Figure 22: A front view of Mach=2.8 isosurface showing the double transition phenomenon. This is for $M_\infty = 2.9$ .....	28
Figure 23: A side view of Mach number contours on the vertical symmetry plane for $M_\infty = 3.1$ . ....	29
Figure 24: Starccm+ images, for the halves of the two wedges, of an isosurface of Mach 2.9, for $M_\infty = 3.1$ .....	30
Figure 25: Starccm+ images, for half a wedge, of an isosurface of Mach 1, showing the shape of the slip surface for $M_\infty = 3.1$ .....	31
Figure 24 shows the shape of the double transition phenomenon, but in this instance for $M_\infty = 3.1$ . The associated slip stream surface is shown in figure 25.....	31
Figure 26: An oblique shadowgraph picture showing transition from regular reflection to Mach reflection, taken by Skews (2000).....	33
Figure 27: A 3-D Starccm+ projected view of a Mach number isosurface at Mach = 2.9, showing transition from regular reflection to Mach reflection. ....	33
Figure 28: A 3-D Starccm+ projected view of a Mach number isosurface at Mach = 2.9, showing transition from regular reflection to Mach reflection. Simulation ran with a laminar flow. ....	34
Figure 29: A close up of the transition from regular reflection to Mach reflection for figure 26. ....	34



Figure 30: A close up of the transition from regular reflection to Mach reflection for figure 27. ....	35
Figure 31: A flooded plan view of Mach number plotted on the horizontal symmetry plane. This is for $M_\infty = 3.1$ . ....	36
As mentioned earlier figure 31 is a flooded plot of Mach number plotted on the vertical symmetry plane, whereby Starccm+ is used as the CFD solver. ....	36
Figure 32: A flooded plan view of Mach number plotted on the vertical symmetry plane. This is for $M_\infty = 3.1$ . ....	37
Figure 33: A flooded plan view of density plotted on the horizontal symmetry plane. This is for $M_\infty = 3.1$ . ....	38
Figure 34: Orthogonal shadowgraph showing the single transition phenomenon. This picture is the same figure 8, but rotated by $180^\circ$ for easy comparison with figure 29. Adapted from Brown and Skews (2004). ....	38
Figure 35: A flooded plan view of density plotted on the vertical symmetry plane. This is for $M_\infty = 3.1$ . ....	39
Figure 36: A flooded plan view of pressure plotted on the vertical symmetry plane. For $M_\infty = 3.1$ . ....	40
Figure 37: A front view of Mach=2.9 isosurface showing the right half of the single transition phenomenon with the vertical plane of symmetry to the left. This is for $M_\infty = 3.1$ . ....	40
Figure 38: A close-up of Figure 37. ....	41
Figure 39: A front view of Mach=2.9 isosurface showing the lower half of the single transition phenomenon below the horizontal plane of symmetry. This is for $M_\infty = 3.1$ . ....	42
Figure 40: A plan view showing streamlines paths being affected by going through shock waves. For $M_\infty = 3.1$ . ....	43
Figure 41: A plan view showing streamlines paths being affected by going through shock waves, for both sides of the wedge. For $M_\infty = 3.1$ . ....	44
Figure 42: A side view showing streamlines paths being affected by going through shock waves. For $M_\infty = 3.1$ . streamlines released just below the horizontal plane of symmetry. ....	45
Figure 43: A front view showing streamlines paths being affected by going through shock waves. For $M_\infty = 3.1$ . ....	46

Figure 44: An isometric view showing streamlines paths being affected by going through shock waves. For $M_\infty = 3.1$ .....	47
Figure 44: A flooded plan view of Mach number plotted on the horizontal symmetry plane. This is for $M_\infty = 2.9$ .....	51
Figure 45: A flooded plan view of Pressure plotted on the horizontal symmetry plane. This is for $M_\infty = 2.9$ .....	51
Figure 46: A contoured side view of Pressure plotted on the vertical symmetry plane superimposed with the slip surface, showing the shape of the slip surface viewed from the side. This is for $M_\infty = 3.1$ .....	52
Figure 47: A flooded plan view of Pressure plotted on the horizontal symmetry plane.....	53
Figure 48: A side view showing streamlines (in colour) paths being affected by going through shock waves. For $M_\infty = 3.1$ . Streamlines released just below the horizontal plane of symmetry.....	54
Figure 49: A front view showing streamlines paths (in colour) being affected by going through shock waves. For $M_\infty = 3.1$ .....	54

## Nomenclature

2-D	Two-dimensional
3-D	Three-dimensional
$\alpha_d$	detachment criterion angle
$\alpha_N$	von Neumann criterion angle
$M_\infty$	Free stream Mach number
CFD	Computational fluid dynamics
GB	GigaByte
RAM	Random Access Memory
Fluent	Commercial CFD software
Starccm+	Commercial CFD software

## Introduction

When an object moves through a gas (for instance air) regardless of whether the gas is stationary or has a velocity of its own, there are pressure pulses emanating from the gas particles immediately on the surface of the object in motion. These pressure pulses travel from the surface of the object at the speed of sound in all directions. This is a mechanism by which a gas continuum is aware of the presence of a solid object. Thus if one were to visualise the streamlines of the gas continuum using smoke for instance, one would see streamlines bent close to the object and further away from the object.

The above scenario is true for a gas if its speed relative to the object is below the speed of sound, which is the speed at which the pressure pulses travel.

For a scenario where the speed of the gas relative to the object is faster than the speed of sound, the gas continuum is no longer getting information from the pressure pulses about the presence of the object, hence cannot get out of the way of the solid object. Given that gas particles cannot simply permeate through the solid surface, nature deals with this conundrum by creating shock waves which bend the gas continuum around the object. Shock waves are discontinuities in the gas continuum, because their thicknesses are in the micrometer region and gas properties are discontinuous from one side of the shock wave to the other side as the gas goes through the shock wave.

Now these shock waves that get generated off the surfaces of objects can be understood as being infinitely thin surfaces that can be plane or curved. These shock waves expand outwardly in their breadth and length; hence they can encounter other objects in the gas continuum. When shock waves encounter surfaces they reflect off the surface, and the pattern of their reflection is dependent on their incoming angle, the flow speed, the boundary layer parameters and the orientation of the reflecting surface.

There are generally two types of reflection patterns, namely: Regular reflection where the shock wave reflection can be likened to that of a light

beam bouncing off a flat surface, and Mach reflection where the incident or incoming shock wave does not come into contact with the reflecting surface, but the incident shock wave seems to bounce off just above the surface with a Mach stem (surface in 3D) developing between the triple point (line in 3D) and the reflecting surface. The triple point is where the incident, reflected, and Mach stem shocks meet. The regular reflection pattern is represented in figure 1, whereas the Mach reflection pattern is represented in figure 2.

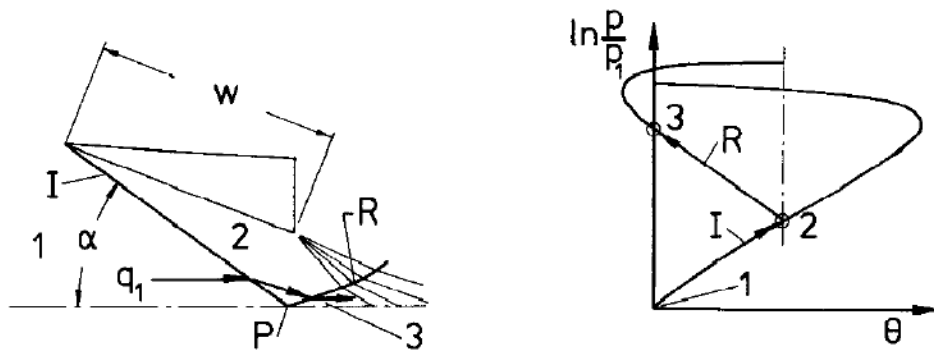


Figure 1: Regular reflection in steady state flow. Physical (left) and shock polar (right). Adapted from Hornung (1986).

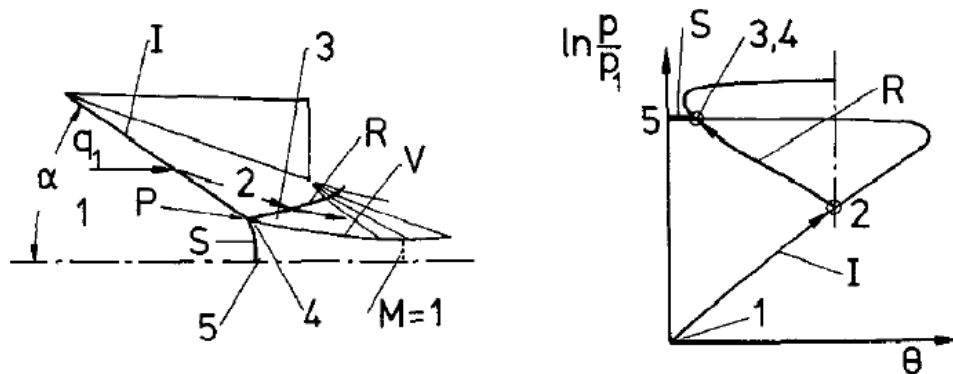


Figure 2: Mach reflection in steady state flow. Physical (left) and shock polar (right). Adapted from Hornung (1986).

The numbers 1 to 5 represent flow regions with different flow conditions. Region 1 has the free stream conditions, i.e. undisturbed flow. Region 2 has the flow that has been deflected by the incident shock wave 'I', by an amount equivalent to the angle of the wedge. Region 3 has the flow that has been deflected by the reflected shock wave 'R'. Region 4 has the flow that has been slowed down to subsonic speed by the Mach stem 'S'. The number 5

simply represents the point where the Mach stem touches the plane of symmetry of the reflecting surface. 'P' is the triple point, 'V' is the shear layer (or the vortex sheet), 'q<sub>1</sub>' is the streamline and 'α' is the incident shock wave's angle with respect to the plane of symmetry. 'M=1' is the Mach number equaling the local speed of sound when the flow in region 4 is accelerated. The flow acceleration occurs because as the shear layer curves towards and then away from the plane of symmetry, a converging-diverging nozzle is formed.

The shock polars in figures 1 and 2 represent what happens physically by relating the pressures in the different regions to the deflection angles the flows in each of the regions go through. 'P' represents a region's pressure and 'P<sub>1</sub>' represents the pressure in region 1. Therefore the vertical axis is the natural log of the ratio of the local region to that of region 1. 'Θ' is the deflection angle of the flow in a region. The deflection angle of region 1 is zero because the flow in this region is at free stream conditions. The deflection angles of the other regions are determined relative to that of region 1. Note that the deflection angles and pressures of regions 3 and 4 is the same. This so because both pressure and deflection angle do not change across the shear layer.

Flow speed behind the reflected shock wave in a regular reflection pattern is still supersonic, whereas the flow field behind the reflected shock wave in a Mach reflection pattern is also supersonic, but the flow field behind the Mach stem is subsonic.

Depending on the reflection pattern that results from the shock wave's encounter with the reflecting surface, the flow speed behind the reflection configuration could be supersonic or a mixture of supersonic and subsonic, with a shear layer separating the two.

Since the reflection pattern can be affected by the flow speed, orientation of the reflecting surface, the angle of the incident or incoming shock wave, then

if any of those parameters were to change after the reflection pattern has been established, the reflection pattern could change from say regular reflection to Mach reflection or vice versa. The nature and the conditions under which this change or transition in reflection pattern is of importance in better predicting the flow speed expected when there are shock wave reflections in the flow field.

When the shock wave happens to be a strong shock wave and with the combination of the above mentioned parameters, one either gets a shock wave angle that is less than the von Neumann angle, greater than the detachment angle or falls in a region between the two angles. The von Neumann and detachment angles are represented in figures 3 and 4 respectively.

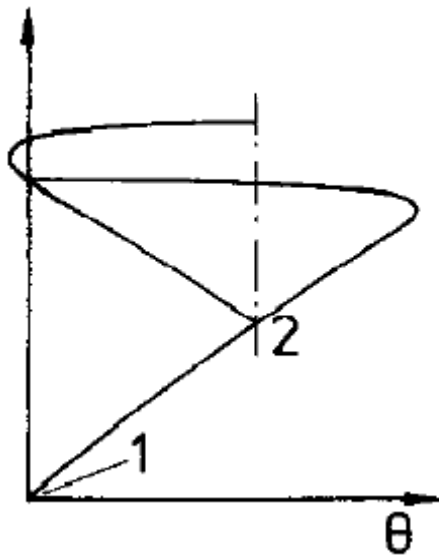


**Figure 3: A shock polar diagram showing the condition at which the shock wave angle is the von Neumann angle.**

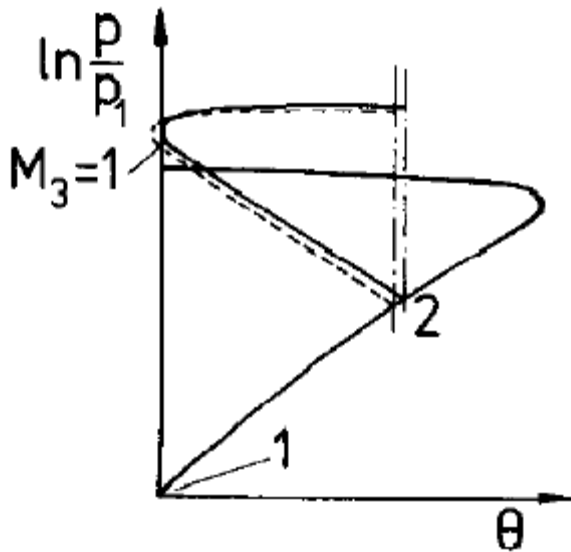


Figure 4: A shock polar diagram showing the condition at which the shock wave angle is the detachment angle (solid line) or the sonic angle (dashed line).

Ben-dor et al. (2001) describe the von Neumann (also known as the mechanical equilibrium) angle as occurring when the reflected shock polar intersects the vertical axis at exactly the normal shock point of the incident shock polar. The von Neumann angle marks the shock wave angle above which if one were to keep the Mach number constant whilst increasing the shock wave angle, one moves to a case where both regular and Mach reflections are possible from a case where only regular reflection is possible.

Ben-dor et al. (2001) also describe the detachment angle as occurring when the reflected shock polar is tangent to the vertical axis. The detachment angle marks the shock wave angle below which if one were to keep the Mach number constant whilst decreasing the shock wave angle, one moves to a case where both regular and Mach reflections are possible from a case where only Mach reflection is possible. It can be seen from figure 4, that the detachment and sonic angles are very close to each other. So for all practical purposes the detachment and sonic angles are treated as one.

The above description is best illustrated in figure 5.

When the shock wave angle is less than the von Neumann angle, one gets regular reflection of the shock wave, reflecting off the surface, and if the shock



wave is at greater than the detachment angle one gets Mach reflection of the shock wave. If the shock wave falls in the region between the two angles, one either gets regular reflection or Mach reflection. The region between the two angles is called the dual solution domain. The above description is illustrated in figure 5 where a shock wave angle is plotted against Mach number.

What figure 5 indicates is that when you start with regular reflection and then keep the Mach number constant while increasing the angle that the flow must turn, one will move into the dual solution domain, but the reflection pattern will remain regular.

For the case where one started with Mach reflection but kept the Mach number constant and reduced the angle that the flow must turn, one would move into the dual solution domain yet remaining with the Mach reflection pattern.

What one can also deduce from the figure 5 is if one were to keep constant the angle that the flow must turn through, but increase the free-stream Mach number, which decreases the shock wave angle, one would move into the dual solution domain whether one started with regular or Mach reflection, but would remain with the reflection pattern that one started with.

Unfortunately this is only true if one assumes that the flow field is two-dimensional, whereas in reality the flow field is generally three-dimensional. The two-dimensional flow field to which figure 5 is applicable can be approximated.

For three-dimensional flow fields one looks at the span of the body encountered by the flow, the span being in the transverse direction to the stream-wise direction. If the span of the body is small as compared to the length of the body in the stream-wise direction, three-dimensional effects creep in and the predictions of figure 5 may not necessarily be true.

But as mentioned above, two-dimensional flow fields can be approximated. This can be achieved by having a span that is much bigger than the length, where the flow in the middle of the body is essentially two-dimensional with

three-dimensional effects not having any effect. But three-dimensional effects will still affect the flow near the edge of the body's span.

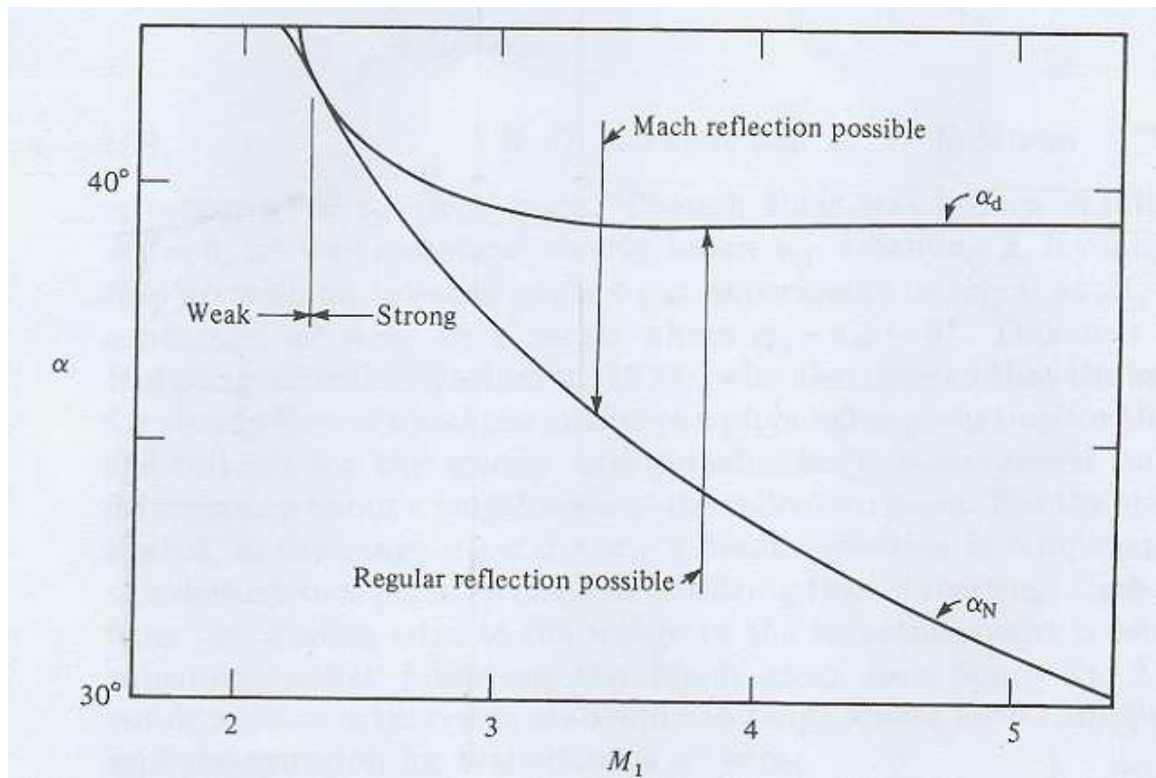
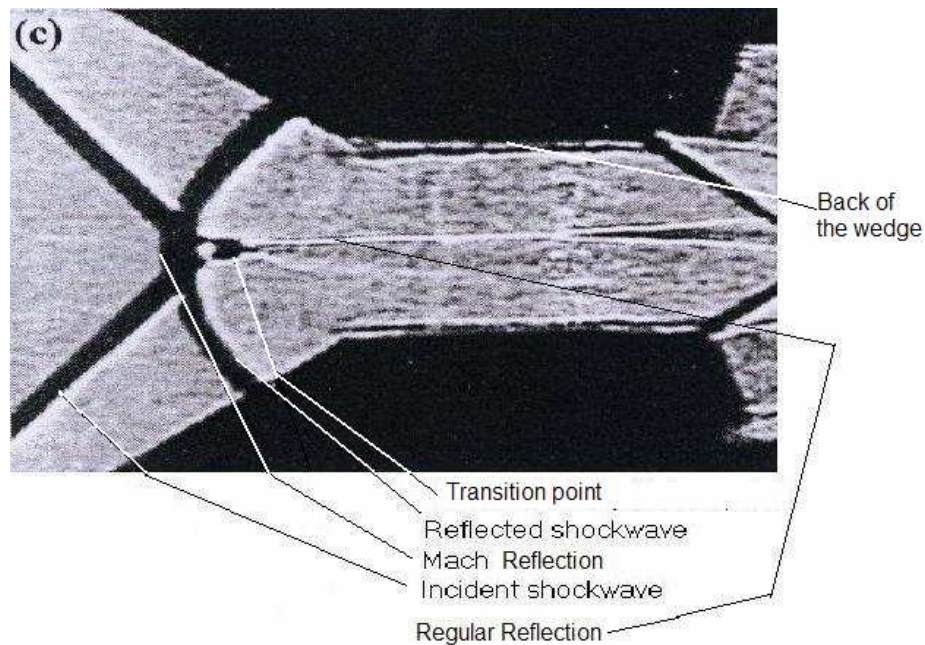


**Figure 5: The von Neumann and detachment criteria as functions of Mach number for a specific-heat ratio of 1.4, where  $\alpha_d$  is the detachment criterion angle,  $\alpha_N$  is the von Neumann criterion angle and  $\alpha$  is the incident shock wave angle.**

## Background and literature review

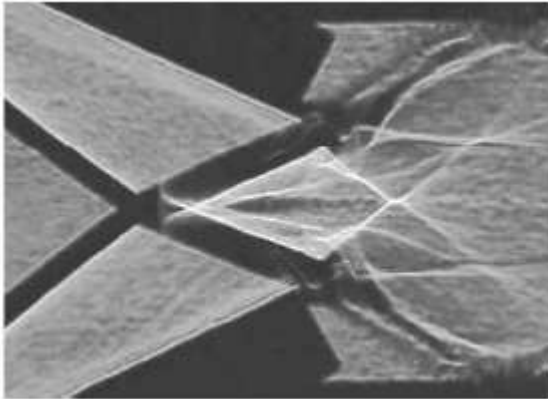
Henderson & Lozzi (1975) found that the detachment criterion for transition was wrong for every flow that they investigated in detail, and these flows include steady, pseudo-steady and unsteady cases. Skews (2000) also support this conclusion, but went a bit further by investigating the flow from a three-dimensional point of view. Skews (2000) took into consideration the effects of the finite wedge edges. The experimentation conducted by Skews (2000) also supported the dual solution phenomenon. Most researchers in their results would observe the dual solution, where they concluded that either RR or MR could occur. But Skews (2000) showed that both types of reflections, i.e. the RR and MR do occur at the same time in the same flow. One of the aims of the present study is based on the work done by Skews (2000).

Figure 6 shows the reflection transition phenomena observed by Skews (2000).



**Figure 6: An oblique shadowgraph picture showing transition from regular reflection to Mach reflection, taken by Skews (2000).**

Irving-Brown and Skews (2004) also show experimental results of the same wedge arrangement as that of figure 6, and these results are shown in figures 7 and 8.



**Figure 7: Conventional shadowgraph showing regular reflection. Adapted from Irving-Brown and Skews (2004).**

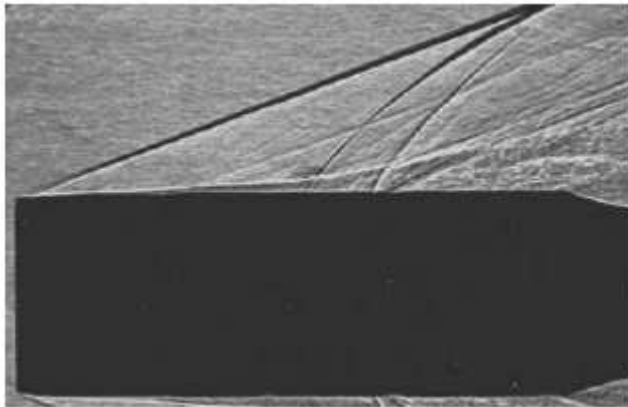


**Figure 8: Orthogonal shadowgraph corresponding to figure 7. Adapted from Irving-Brown and Skews (2004).**

Ivanov et al. (1999) used a laser sheet vapour screen technique to visualise the 3D structure of a shock wave reflection in wind tunnel experiments with symmetrical wedges. A new shock reflection configuration was observed. For this configuration when moving along the span-wise direction, the Mach reflection existing in the central plane is changed into regular reflection and later again the peripheral Mach reflection appears. Figure 9 shows the reflection transition phenomena observed by Ivanov et al. (1999).

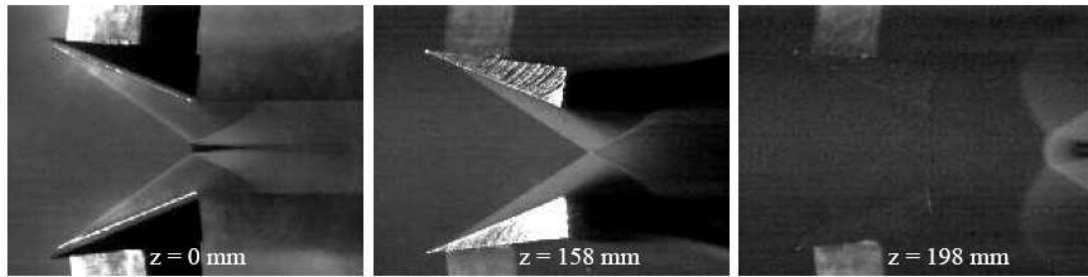


**Figure 9: Laser sheet images at different span-wise positions ( $z$ ) taken by Ivanov et al. (1999).**

Sudani et al. (2002) conducted experiments for an asymmetric arrangement and also managed to observe the same phenomena observed by Ivanov (1999), and these observations are shown in figure 10.

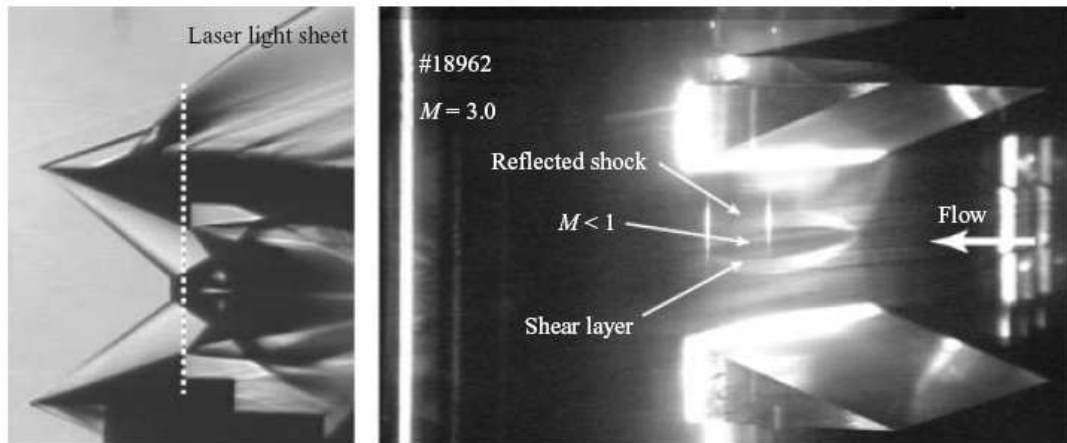


**Figure 10: Schlieren and vapour-screen pictures in the asymmetric arrangement.  $M_\infty=3.0$ . Adapted from Sudani et al. (2002).**

Sudani et al. (1999) conducted experimental studies of shock wave reflections in steady flows at Mach numbers of 3 to 4 in a blow-down supersonic wind tunnel. In a symmetric arrangement where the upper wedge is vertically moved with its deflection angle fixed, the transition to Mach reflection occurred at a certain location when the inlet aspect ratio was increased, hence no significant effect of inlet aspect ratio on the transition location could be observed. Vapour screen visualisation technique was used for the experimental studies and it was found that the Mach stem has its maximum height at the span-wise centre and that three-dimensional effects promote regular reflection. Their experimental data led to the hypothesis that wind tunnel disturbances cause the transition to Mach reflection in the dual-solution domain.

However Kudryavtsev et al. (2002) have concluded, through the use of numerical simulations, in the dual solution domain Mach reflection was more stable than regular reflection. They established this through the use of what they call free-stream disturbances.

As for the effects coming from downstream flow conditions on the Mach stem height, Chpoun and Leclerc (1999) show that there is none. This is illustrated in figure 11 where experiments were conducted at hypersonic conditions on wedges with various trailing edge corner angles. The figure shows wedges with the same wedge angle, but the trailing edge corner angle varies from  $45^\circ$  up to  $145^\circ$ . As is pointed out in Chpoun and Leclerc (1999) this observed phenomenon contradicts some analytical findings.

Hornung (1986) concludes that the expansion wave coming from the trailing edge of the wedge causes the slip stream to curve away from the horizontal symmetry plane, thereby forming the diverging-converging nozzle. Because up until the throat of the nozzle the flow is subsonic, Hornung (1986) concludes that an information pathway is created back to the triple point.

Henderson et al. (2001) make the point that by definition regular reflection has no boundary layer interaction, therefore a shock wave reflection off a plane of symmetry will always give either regular reflection or Mach reflection. On the contrary, precursor regular reflection always appears with boundary layer interaction, as on a ramp surface.

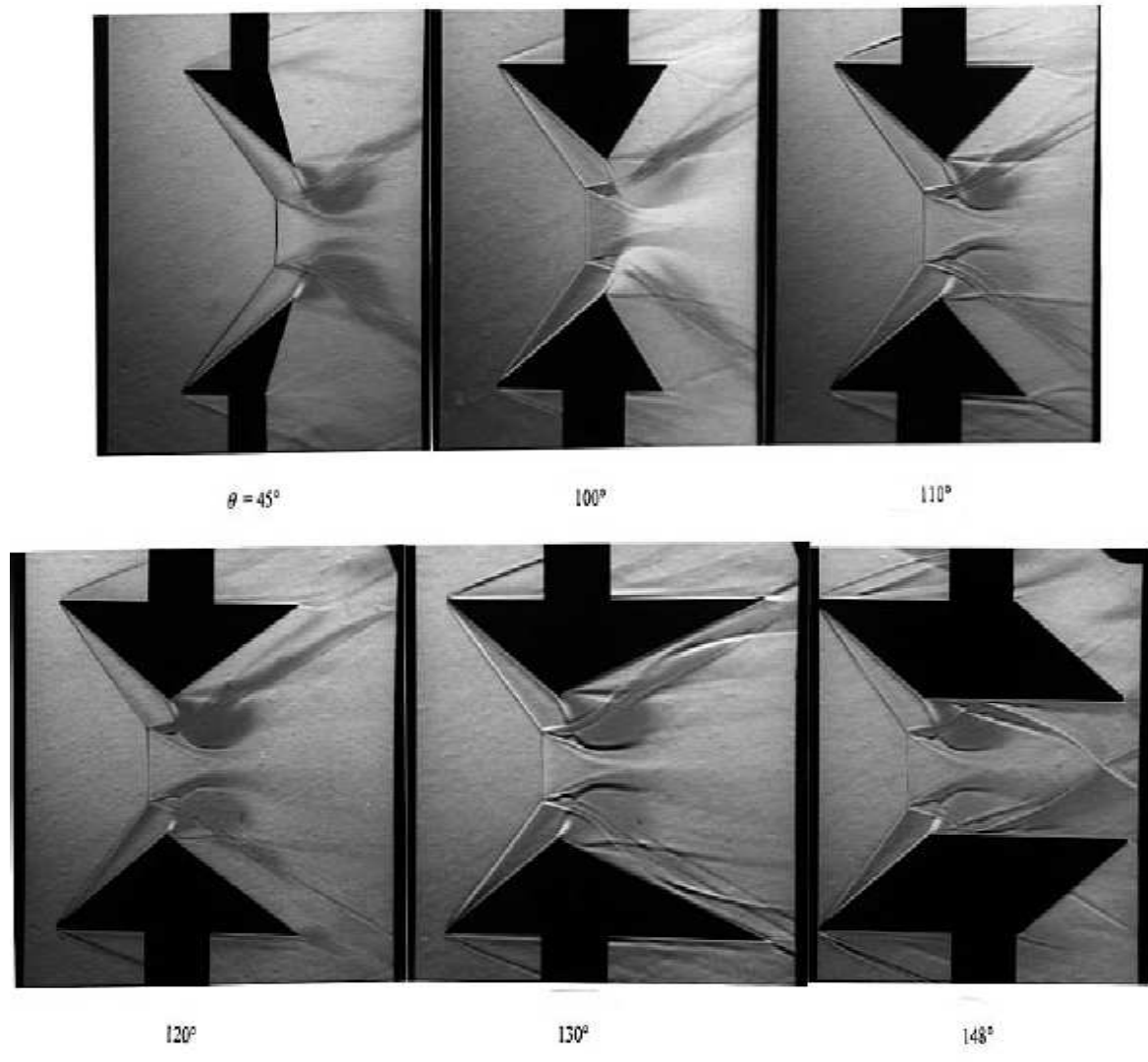


Figure 11: shadowgraph pictures showing the absence of influence on the Mach stem height by downstream flow conditions. Adapted from Chpoun and Leclerc (1999).

## Objectives

The first aim of this project is to carry out simulations of experiments conducted independently by Ivanov et al. (1999) and Sudani et al. (1999) on shock wave interaction of two incident shock waves generated by two symmetrically arranged wedges. The wedges have a high aspect ratio, i.e. the ratio of the width to the length, which eliminates three-dimensional effects at the model centre line. For this setup, the shape of the reflected shock waves at the model centre is not curved, but flat.

The reflection pattern observed by both teams is a Mach reflection at the model centre line and regular reflection as one moves towards the edge of the model. However, further out the reflection pattern transitions to Mach reflection and remains so, as expected, with a peripheral Mach reflection pattern.

The second aim is to conduct simulations at lower Mach numbers with the intent to reproduce the reflection patterns observed by the two above-mentioned teams. Thereafter experiments will be conducted at Mach 3.3 in the supersonic wind tunnel at University of the Witwatersrand.

The third aim is to analyse the complete flow structure from both the experimental and computational simulation point of view, to determine the effect of changing the geometrical set-up on the reflection pattern.

The fourth aim is numerically resolve the sudden change in height of the Mach stem at the transition point from regular reflection to Mach reflection observed by Skews (2000).



## **Method and procedure**

The research project follows work done by the candidate on a fourth year research project in which the fourth aim of this proposal was the main aim. The title of the fourth year research project was 'The Numerical investigation of the instability of the mechanical equilibrium point'. Although retrospectively this title is incorrect since the talk of a mechanical equilibrium point only applies when one assumes a two-dimensional flow field. The method used for the investigation for this fourth year project was a commercial Computational Fluid Dynamics (CFD) software package named STAR-CD.

Subsequent to the fourth year project, preliminary work had been done in investigating some of the objectives of the current project. In this preliminary work Fluent, another commercial CFD software package was used. These two works were used as the basis from which this current project would be carried out.

## ***Case descriptions***

The above stated objectives describe different shock wave reflection phenomena occurring under different free stream Mach numbers and geometric configurations. The first and second objectives were investigated using a case with a geometric configuration having big transverse dimensions relative to those in the streamwise direction. This case meant for the investigation of the first and the second objectives will be called Double transition Case.

The fourth objective was investigated using a case with a geometric configuration having small transverse dimensions relative to those in the stream wise direction. This case meant for the investigation of the fourth objective will be called Single transition Case.

Each of these cases will be described separately in the following sections.

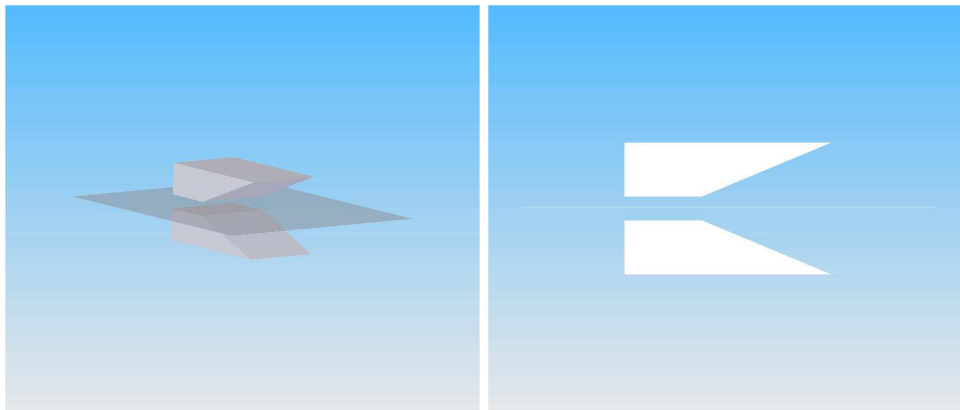
## Single transition Case

The geometric setup in the investigation of transition from regular reflection to Mach reflection consists of two symmetrically arranged wedges with finite spans with one placed above the other. This arrangement results in the same reflection outcome as would have been achieved with using a wedge and a flat surface parallel to the horizontal. But the advantage of using this outlined setup is that one completely removes the affect of a boundary layer on the reflection pattern. Hence one has a virtually perfect adiabatic surface.

Because the wedges are symmetrically arranged about the perfect reflection surface, one can assume symmetry and use only one wedge. Symmetry also exists about the centre plane of the wedge span; hence half a wedge is used in the CFD simulations.

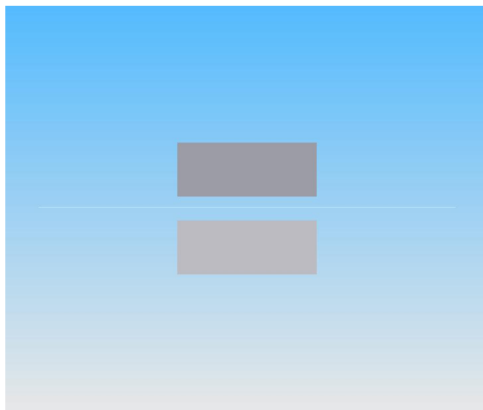
For this case where the span of the wedge is small in comparison to the length of the wedge, in this case span to length ratio, called the aspect ratio, of 0.5 ( a span of 20 mm and a length of 40 mm), the trailing edge gap is 9 mm with a wedge angle of 25°. This case is a numerical replication of work carried out by Skews (2000) and Skews et al. (2004), where a blow-down wind tunnel with a cross section of 100 mm x 100 mm was used at  $M_\infty = 3.1$ , hence the tunnel wall is modelled to be 50 mm away from the centre of the wedge.

Pictures showing the geometric setup of the wedges are shown in Figure 12.



**Isometric view**

**Side view**



**Front view**

**Figure 12: Pictures showing arrangements of the two wedges used in the Single transition case.**

### **Double transition case**

The geometric configuration for this case is the same as that for the single transition case.

For a case where the span of the wedge is large in comparison to the length of the wedge, the aspect ratio is 3.75 with a span of 300 mm and a length of 80 mm, the trailing edge gap of 24 mm and a wedge angle of  $21.4^\circ$ . This case is a numerical simulation of the work carried out by Ivanov et al. (1999) using a wind tunnel with a cross section of 600 mm x 600 mm at free stream Mach number of 4. The tunnel wall was modelled to be 300 mm away from the centre of the wedge.

Pictures showing the geometric setup of the wedges for this case are shown in Figure 13.

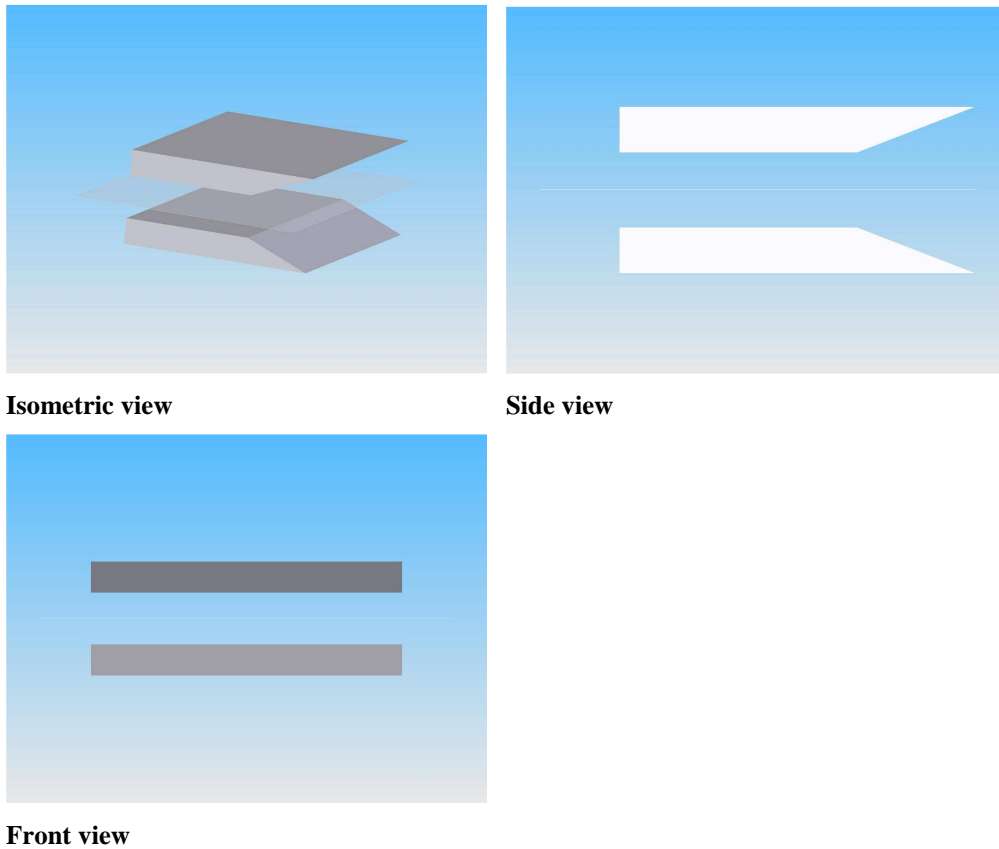


**Figure 13: Pictures showing arrangements of the two wedges used in the Double transition case.**

Detailed drawings showing dimensions of the wedge setups for both cases are in Appendix C.

Fluent and Starccm+, two commercial CFD codes, were used for the simulations. In all the simulations inviscid flow was assumed, except in one instance for the single transition case where a laminar flow was assumed in order to evaluate whether there are any viscous effects. The mesh generated in Gambit was imported into both Fluent and Starccm+, but refinement was done using Fluent. This refinement was done based on density gradients, and it was done until refinement could be done any longer. The refined mesh was then also used in Starccm+ although without the benefit of an initial solution to start from. For both Fluent and Starccm+ a coupled (density based) solver was selected. This is because coupled solvers are very good at resolving

discontinuities like shock waves in flows. For Fluent, a second-order upwind spatial discretisation scheme with a Roe-Flux Difference splitting (FDS) limiter was used because it works well in flows with discontinuities. Algebraic Multigrid method with V-cycle was used to speed up the simulation while not affecting accuracy of the results. Adaptation was done resulting in over 1.84 million cells for the Single transition Case and over 1.7 million cells for the Double transition Case.

All the codes were ran on 64-bit Linux servers, with any server having up to 8 GB of RAM, and the option of parallelising the simulations on up to 24 computers.

## Discussion of results

### *Double transition Case*

For the case with a wedge aspect ratio of 3.75, the results presented are from both Fluent and Starccm+ although the former code's results are for a Mach number of 4.0 and the latter code's results are for Mach numbers of 3.1 and 2.9.

As stated in the first objective in the objectives section, Ivanov et al. (1999) experimentally observed a very interesting reflection phenomenon, where there is Mach reflection observed at the centre of the wedge which transitions to regular reflection as one moves towards the tunnel wall. But as expected the regular reflection transitions to a peripheral Mach reflection as one move further towards the tunnel wall. Ivanov et al. (1999) ran their experiments at Mach number 4.0.

The shock wave reflection transition phenomenon is very interesting because in the literature the focus is on establishing the transition criterion from regular reflection to Mach reflection and vice versa. And this is done from the perspective of the flow being view or assumed to be two dimensional or pseudo-two dimensional. From this observed shock wave reflection transition phenomenon (i.e. observed by Ivanov et al. (1999)) it can be seen that although the flow is essentially two dimensional at the centre of the geometric setup, the reflection pattern changes from Mach reflection at the centre as one moves outwards from the centre. The Mach surface (Mach stem in two dimensions) narrows in height up to the point where there is transition from Mach reflection to regular reflection. At this point at which this transition from Mach reflection to regular reflection occurs, the incident shock wave is still flat and not curved. As one moves further away from the centre the regular reflection persists for a short distance and then there is the expected transition to Mach reflection. Both of these transitions are smooth, which might suggest the stability of the reflection patterns.

It should be mentioned that the Mach reflection at the centre of the geometric setup is as predicted by two-dimensional theory. Then a question naturally arises of why is there transition from Mach reflection to regular reflection if the Mach reflection is as predicted by two dimensional theory, meaning that if all conditions are kept constant then the reflection pattern should be stable and not change. This question could be answered by viewing this as being further evidence that three dimensional effects promote regular reflection over Mach reflection as concluded by Sudani and Hornung (1998).

It is worth noting that in the literature there is no transition criterion for a three-dimensional transition.

As stated above the experiment conducted by Ivanov et al. (1999) was modelled using two commercially available CFD codes. The modelling was conducted at the Mach numbers 4 (the Mach number for the experiment), 3.1 and 2.9. The aim for running simulations at Mach numbers 3.1 and 2.9 was to achieve what is stated in the second objective. The results for the simulation at Mach number 4 are presented in figure 14 below. They clearly agree with the experimental observation made by Ivanov et al. (1999) at those marked stations, presented in figure 15. But the only difference between the two set of results is that the simulation was run as an unsteady one, where the presented results with a double transition fade away and one gets a case with regular reflection at the centre that transitions to the expected peripheral Mach reflection.

This brings one back to the conclusion made by Sudani and Hornung (1998) that three dimensional effects do promote regular reflection over Mach reflection.

But then when one runs the simulations at Mach numbers 3.1 and 2.9 one observes the double transition phenomenon with the simulations being run in a steady state. The results at Mach numbers 3.1 and 2.9 are presented in figures 16 and 17 respectively at the same stations as those of the experiment conducted by Ivanov et al. (1999). The results from the simulations at these two Mach numbers satisfy the second objective of observing the double transition at Mach numbers attainable at the Wits Flow Research Unit facility.

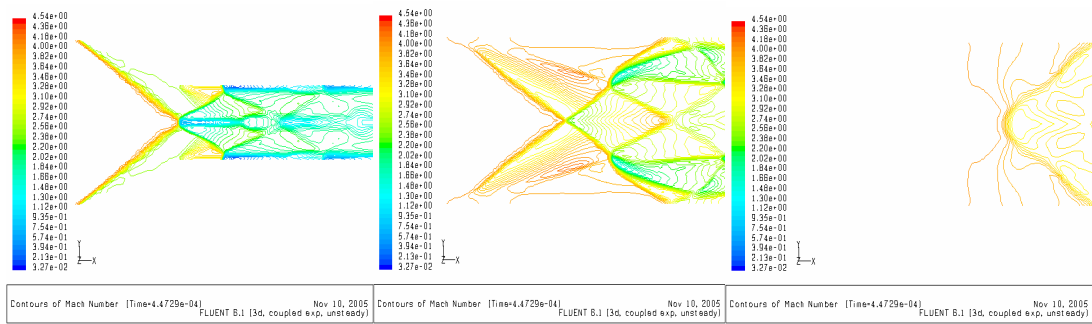


**Figure 14: CFD pictures at span-wise positions ( $z$ ) of, from left to right 0 mm, 158 mm and 198 mm, obtained using Fluent for  $M_\infty = 4.0$ .**

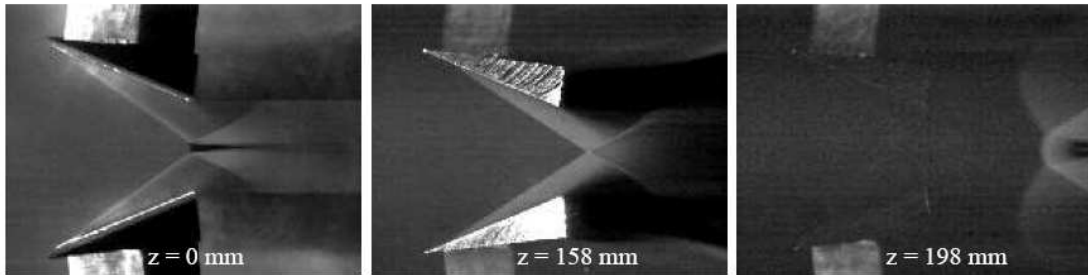


**Figure 14: Laser sheet Images at different span-wise positions ( $z$ ) taken by Ivanov et al. (1999) for  $M_\infty = 4.0$ .**



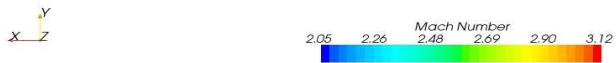
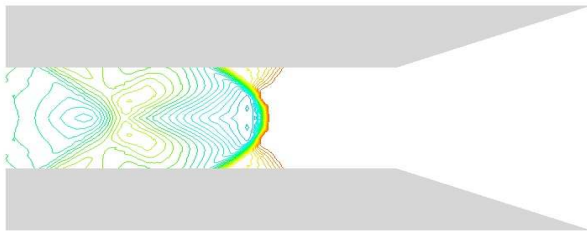
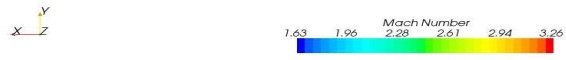
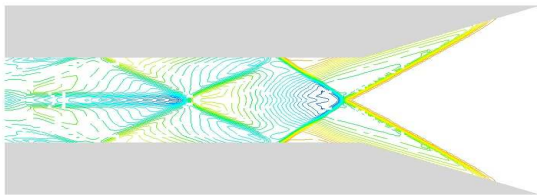
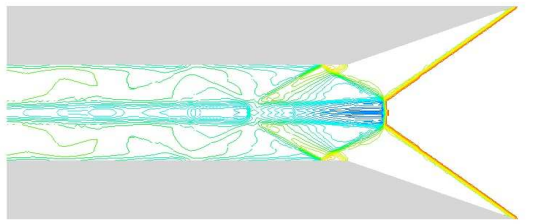


**Figure 16: CFD pictures at span-wise positions ( $z$ ) of, from top to bottom 0 mm, 158 mm and 198 mm, obtained using Fluent for  $M_\infty = 3.1$ .**

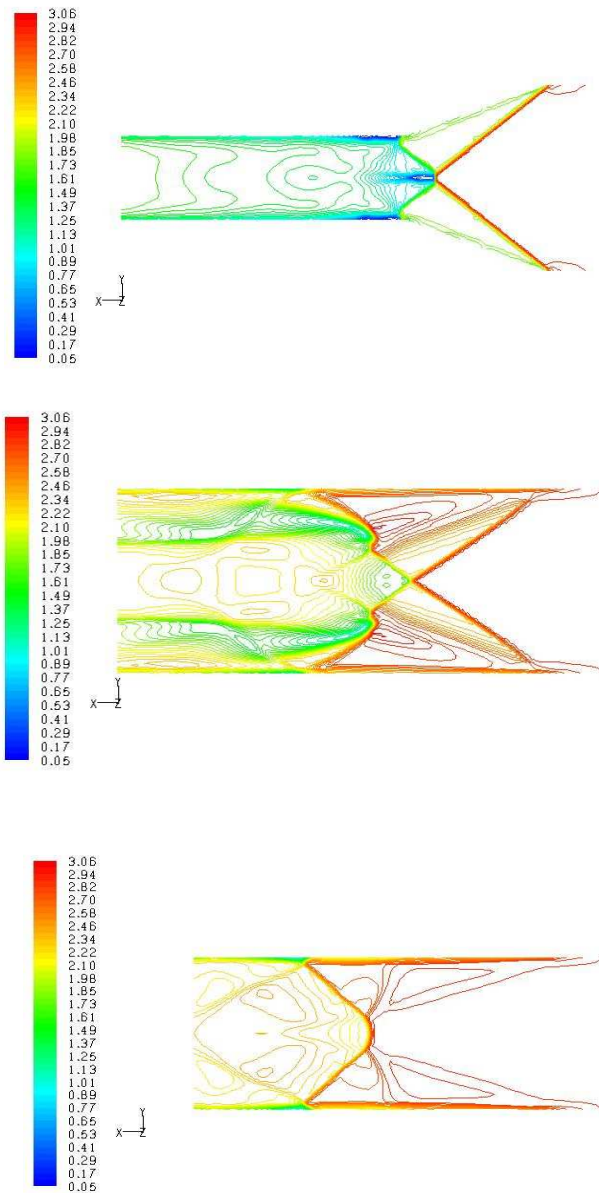


**Figure 17: CFD pictures at span-wise positions ( $z$ ) of, from top to bottom 0 mm, 158 mm and 198 mm, obtained using Fluent for  $M_\infty = 2.9$ .**

In all the simulations inviscid flow was assumed, except in one instance for the single transition case where a laminar flow was assumed in order to evaluate whether there are any viscous effects. The mesh generated in Gambit was imported into both Fluent and Starccm+, but refinement was done using Fluent. The refined mesh was then also used in Starccm+ although without the benefit of an initial solution to start from as in Fluent.

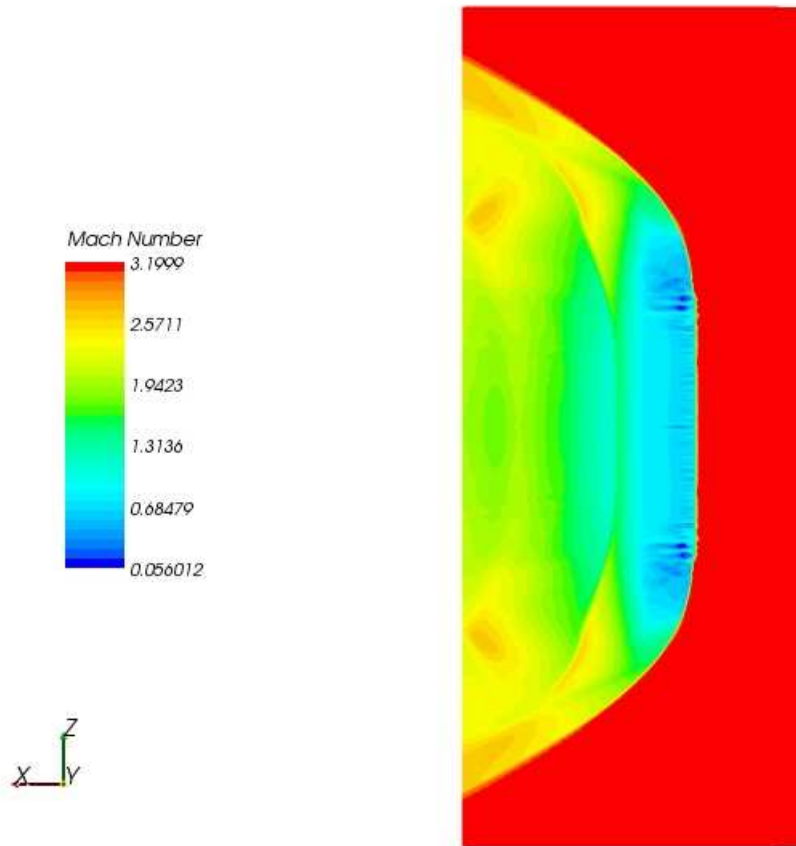


**Figure 18: A flooded plan view of Mach number plotted on the horizontal symmetry plane. This is for  $M_\infty = 3.1$ .**

Figure 18 shows a plan view plot of Mach number from which one can see the subsonic region behind the flat portion of the Mach surface. As stated earlier, for this flat portion two-dimensional theory can predict the reflection pattern. But one can also see the transition from Mach reflection to regular reflection within a small part of the flat portion. This transition can not be predicted by two-dimensional theory. Because the flow coming at the incident shock wave is perpendicular (in a stream wise sense) to the shock wave, and the flow behind the shock wave is supersonic, it can be seen that the reflection pattern is indeed regular.

From Figure 18 one can also see the extent of the subsonic region behind the Mach surface. This subsonic region has the converging-diverging nozzle effect in both the stream wise and lateral direction. The shape of the slip

stream bounding the subsonic region can also be observed from figure 18. There is hardly any change in speed behind the subsonic region.

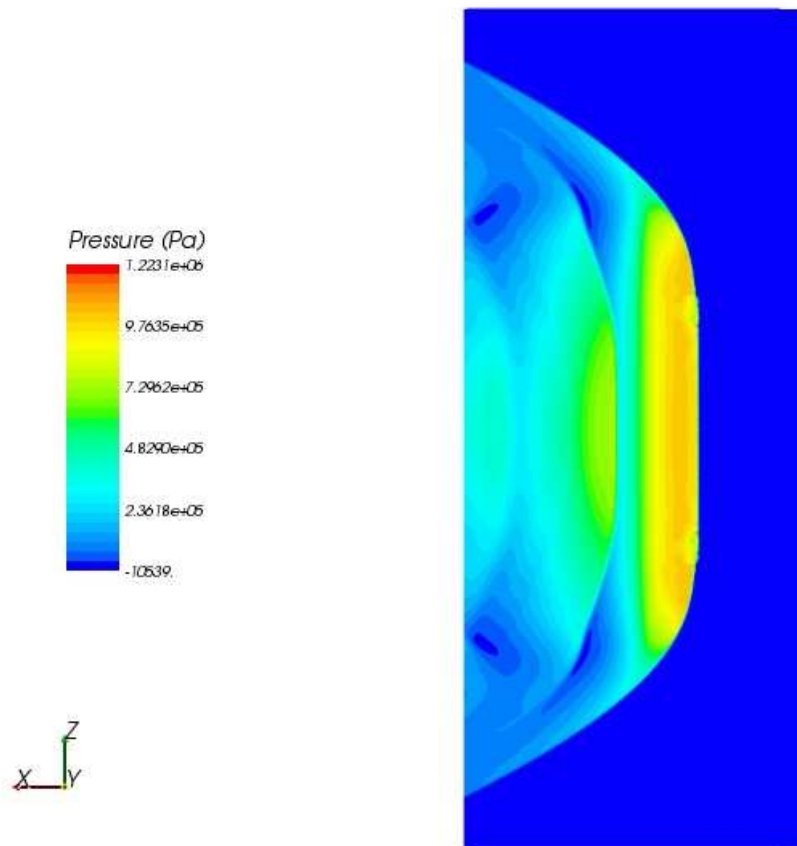


**Figure 19: A flooded plan view of pressure plotted on the horizontal symmetry plane. This is for  $M_\infty = 3.1$ .**

From figure 19 one can see that there is little difference in pressure as one move across the peripheral Mach surfaces. Another observation is that because there is no change in pressure across the slip stream (in three-dimension it becomes a slip surface, refer to figures 20 and 24 for the shape), the shape of the subsonic region as seen in figure 18 can not be observed in figure 19. Instead a strange pressure distribution is observed that can not be correlated with the observed Mach number distribution plotted in figure 18.

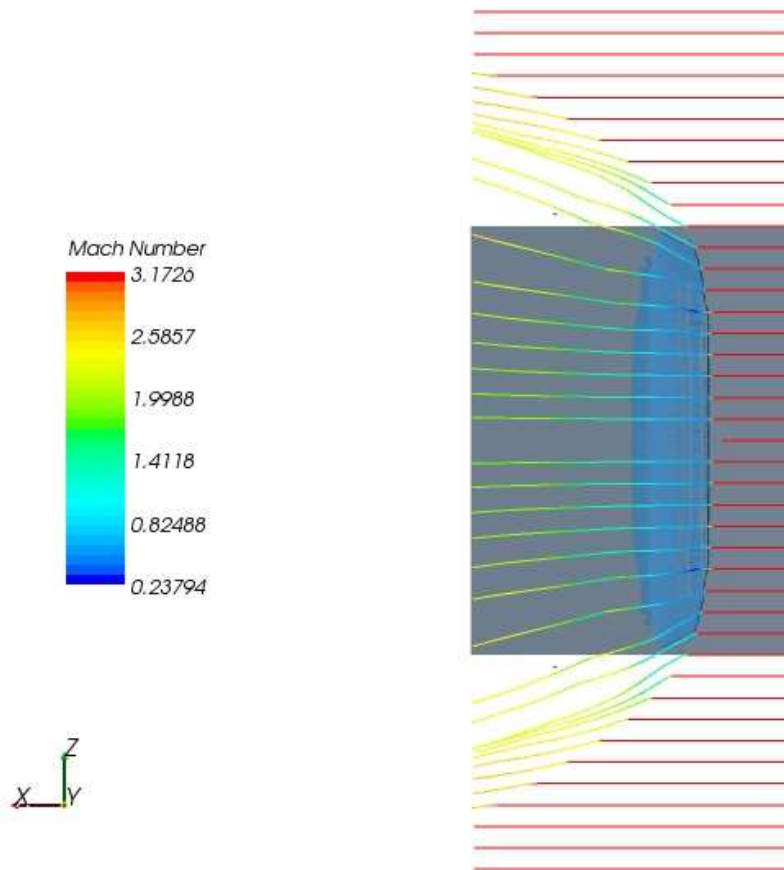


**Figure 20: A plan view plot of a slip surface (shear layer) with streamlines moving from right to left plotted on the horizontal symmetry plane, with the wedge in the background. This is for  $M_\infty = 3.1$ .**

Figure 20 shows how the flow as represented by the streamlines gets affected by the shock system. Figure 20 also shows the plan view of the slip surface (shear layer).

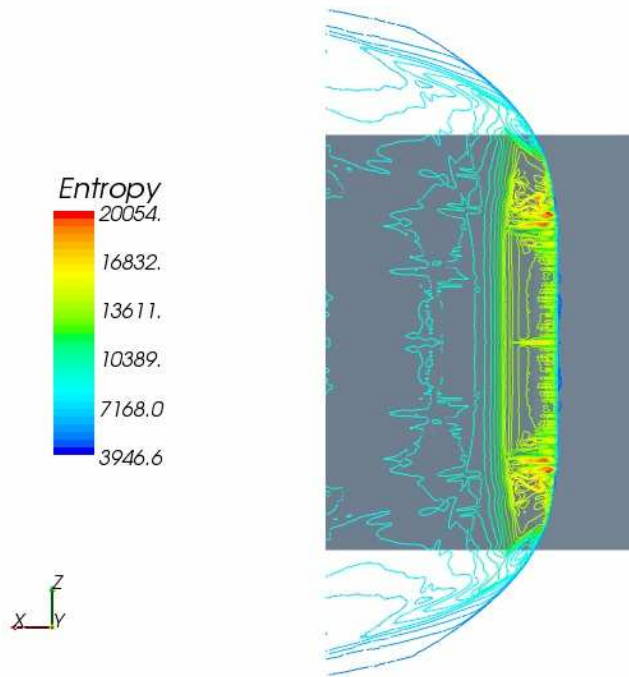


**Figure 21: A plan view plot of entropy on the horizontal symmetry plane. This is for  $M_\infty = 3.1$ .**

Figure 21 shows the increase or production in entropy in the flow behind the incident shock wave and the Mach surface. From figure 21 one can see that the highest production of entropy occurs in the subsonic region. Since the subsonic region is behind the Mach surface, this means there is more energy loss in the flow going through the Mach surface than through two oblique shock waves. This is the only explanation since another way in which entropy could be increased or created is by turbulence, but the flow is modelled as being inviscid. The small region where there is regular reflection the flow goes through the incident and reflected shock waves, but the flow behind them has less turbulence than the subsonic region. Explained another way, if one were to look at the normal components of the incident and reflected shock waves their combined Mach number drop across them is smaller than that across a Mach stem, with the Mach stem being a normal shock wave.

The peripheral Mach surface produces the least amount of entropy because the flow comes at it at an angle. The four small red regions of high entropy are due to part of the Mach surface in front of them being stronger than the rest of the Mach surface and have nothing to do with the transition points. This is easily verifiable when comparing figures 20 and 21 by observing where the subsonic region ends as described by the slip surface.

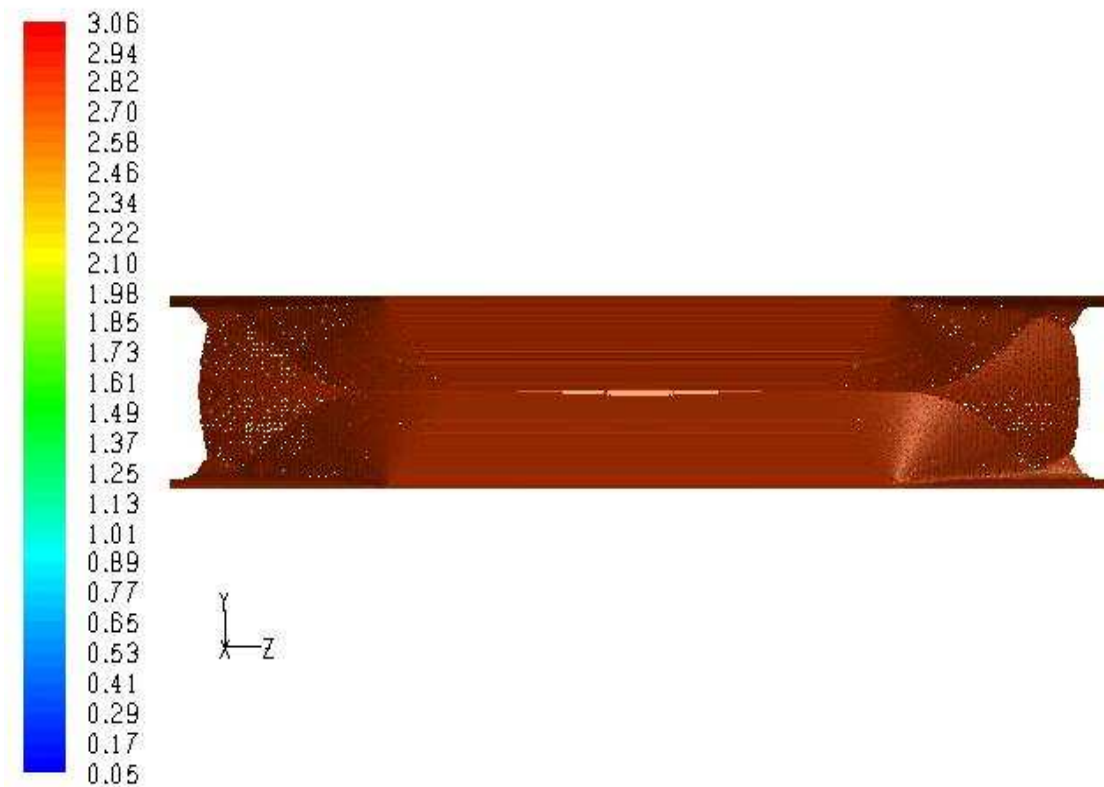


**Figure 22: A front view of Mach=2.8 isosurface showing the double transition phenomenon. This is for  $M_\infty = 2.9$ .**

From figure 22 one can observe the shape of the double transition phenomenon in three dimensions. At the centre of the isosurface is the Mach surface, though small in size. One can easily see the tapering off of the central Mach surface as one moves outwards until there is transition to regular reflection. Then one can definitely see the rapid expansion of the peripheral Mach surface at the edges.

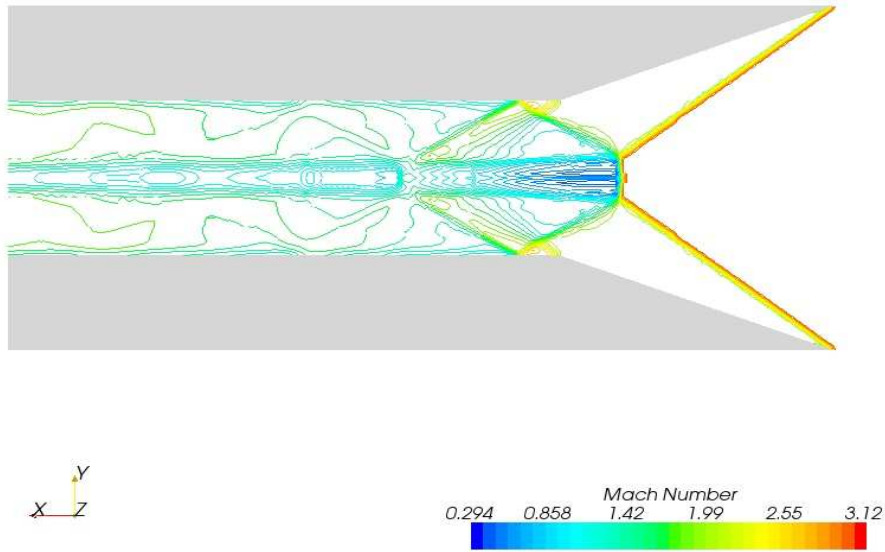
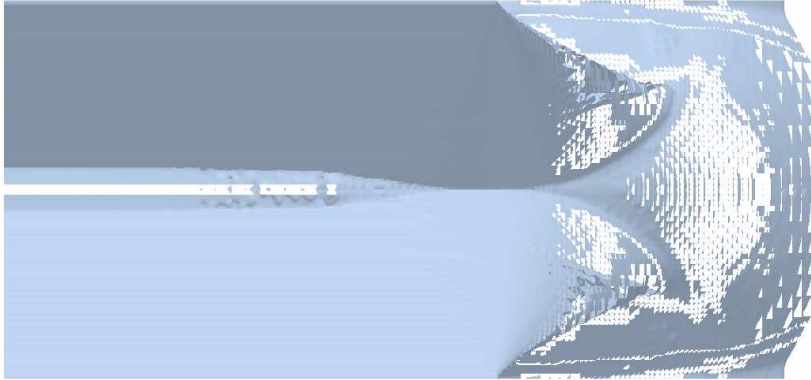


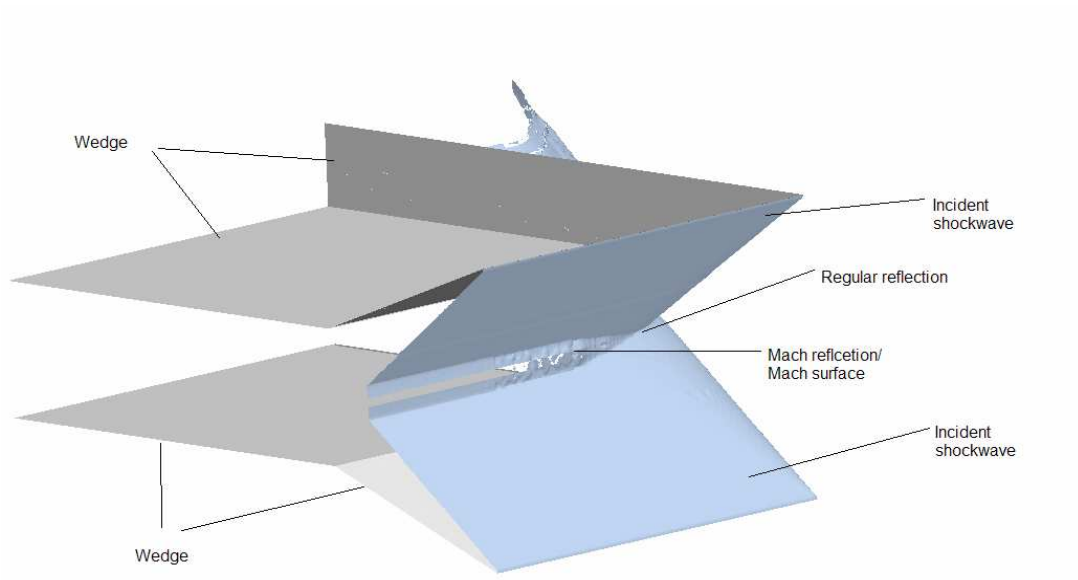
**Figure 23: A side view of Mach number contours on the vertical symmetry plane for  $M_\infty = 3.1$ .**

Prediction by two-dimensional theory applies at the centre of the wedge arrangement. In this case this is illustrated in figure 23 where the Mach reflection observed in the figure is expected, because for this wedge angle and Mach number the reflection pattern falls within the dual solution domain.



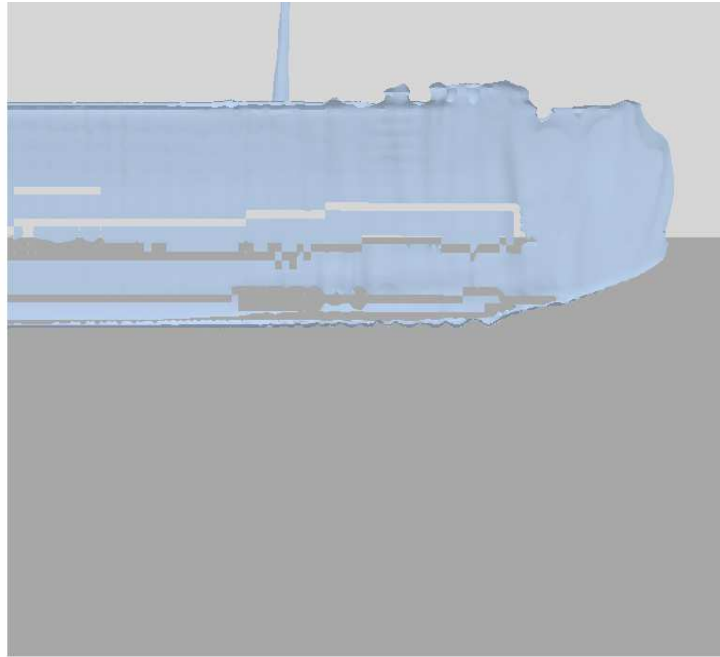


View from the wedge setup inlet

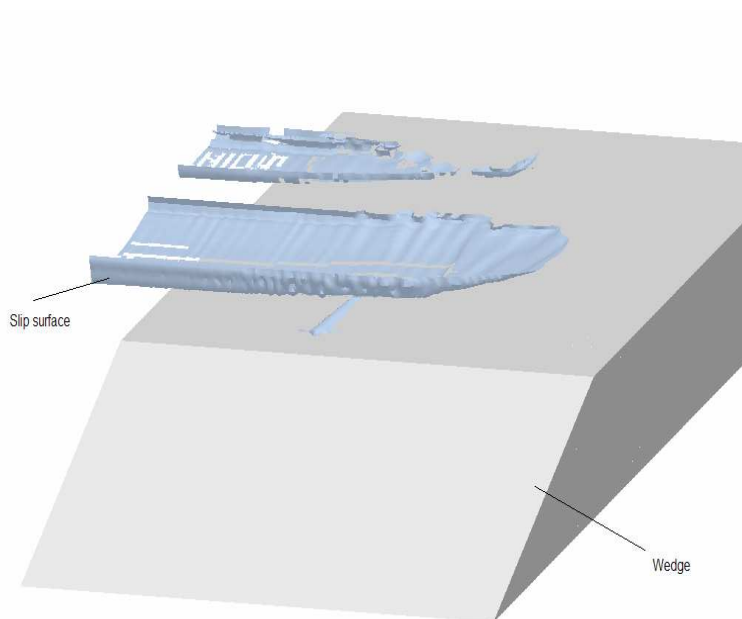


Isometric view of the shockwave reflection

**Figure 24: Starccm+ images, for the halves of the two wedges, of an isosurface of Mach 2.9, for  $M_\infty = 3.1$ .**



Plan view of the slip surface



Isometric view of the slip surface

**Figure 25: Starccm+ images, for half a wedge, of an isosurface of Mach 1, showing the shape of the slip surface for  $M_\infty = 3.1$ .**

Figure 24 shows the shape of the double transition phenomenon, but in this instance for  $M_\infty = 3.1$ . The associated slip stream surface is shown in figure 25.

### ***Single transition case***

As in the double transition case the single transition case simulations were run using both Fluent and Starccm+, but results for a particular flow feature will be presented using pictures from only one of the two packages. Additional pictures of the results will be presented in Appendix B.

Just as it was discussed in the experimental and computational setup sections above, the single transition case objective was examined using a wedge with an aspect ratio of 0.5 and the simplifying assumption made for the double transition case were applied in this case too.

In as far as answering the fourth aim put forward in the objective section, the sudden change in height of the Mach stem at the transition from regular reflection to Mach reflection can not be observed from the simulations of either of the two simulations packages. The reason for this could be that since the wind tunnel used by Skews (2000) was noisy, vibrations in the flow could have triggered the sudden transition from regular reflection to Mach reflection.

This observation is presented in figures 26 and 27 showing the experimental observation made by Skews (2000) and the simulation results obtained by this author using Starccm+, respectively.

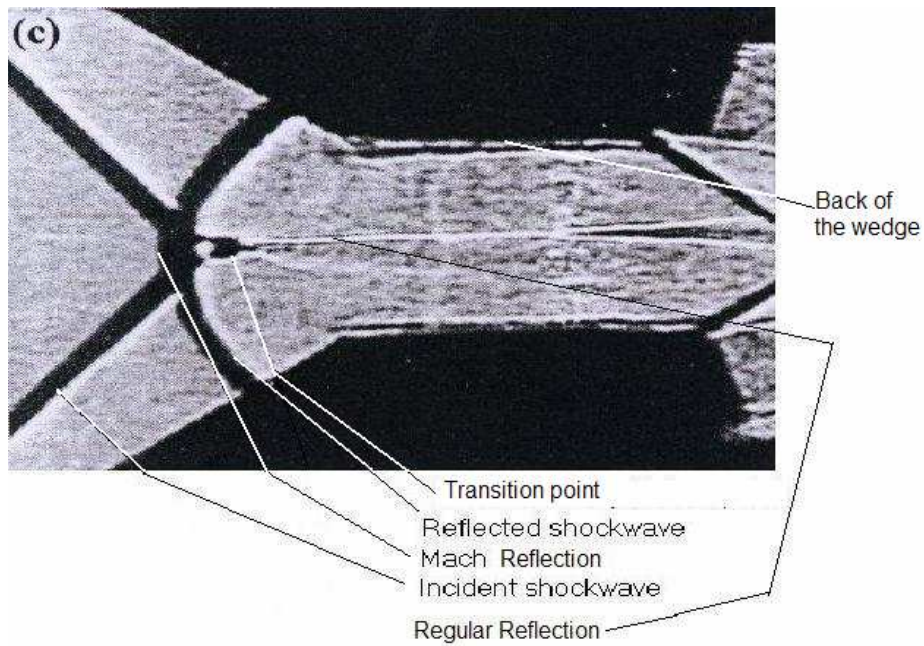


**Figure 26: An oblique shadowgraph picture showing transition from regular reflection to Mach reflection, taken by Skews (2000).**

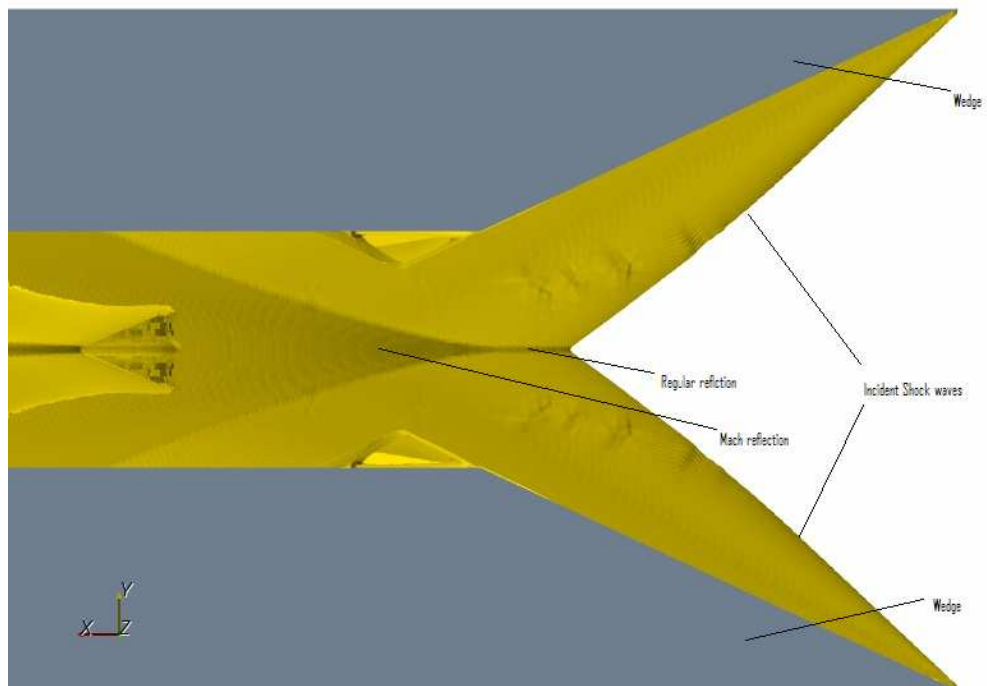


**Figure 27: A 3-D Starccm+ projected view of a Mach number isosurface at Mach = 2.9, showing transition from regular reflection to Mach reflection.**

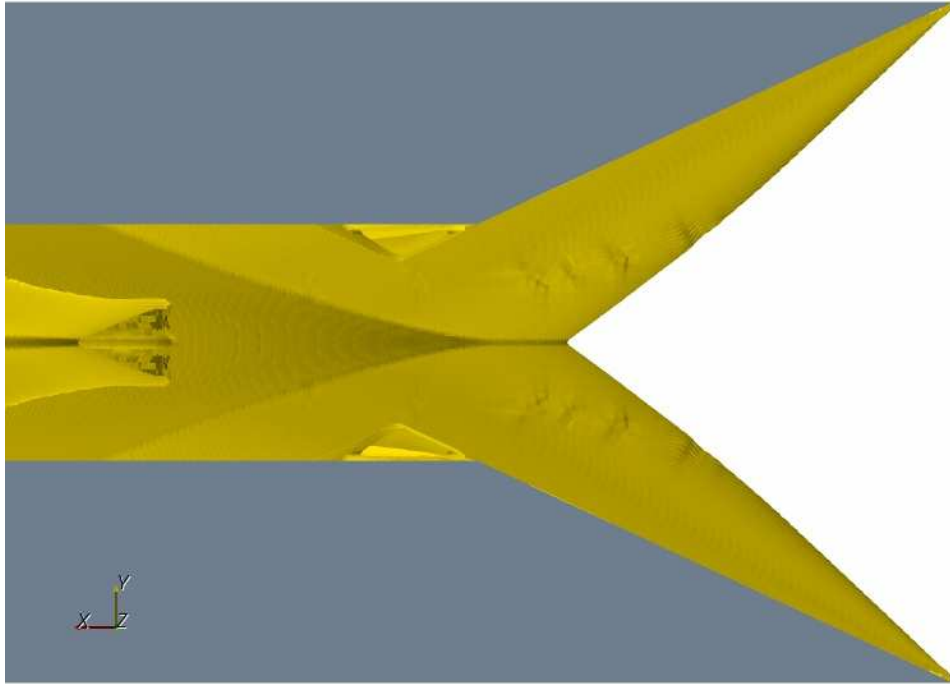


**Figure 28:** A 3-D Starccm+ projected view of a Mach number isosurface at Mach = 2.9, showing transition from regular reflection to Mach reflection. Simulation ran with a laminar flow.



**Figure 29:** A close up of the transition from regular reflection to Mach reflection for figure 26.



**Figure 30: A close up of the transition from regular reflection to Mach reflection for figure 27.**

Figure 28 shows the same view as figure 27, but for a laminar flow. The aim of running a laminar simulation was to see if the sudden jump in the transition from regular reflection to Mach reflection observed by Skews (2000) might be due to viscous effects. As can be from both figures 27 and 28, there is no difference in the flow patterns. Close ups of both figures are presented in figures 29 and 30 respectively.

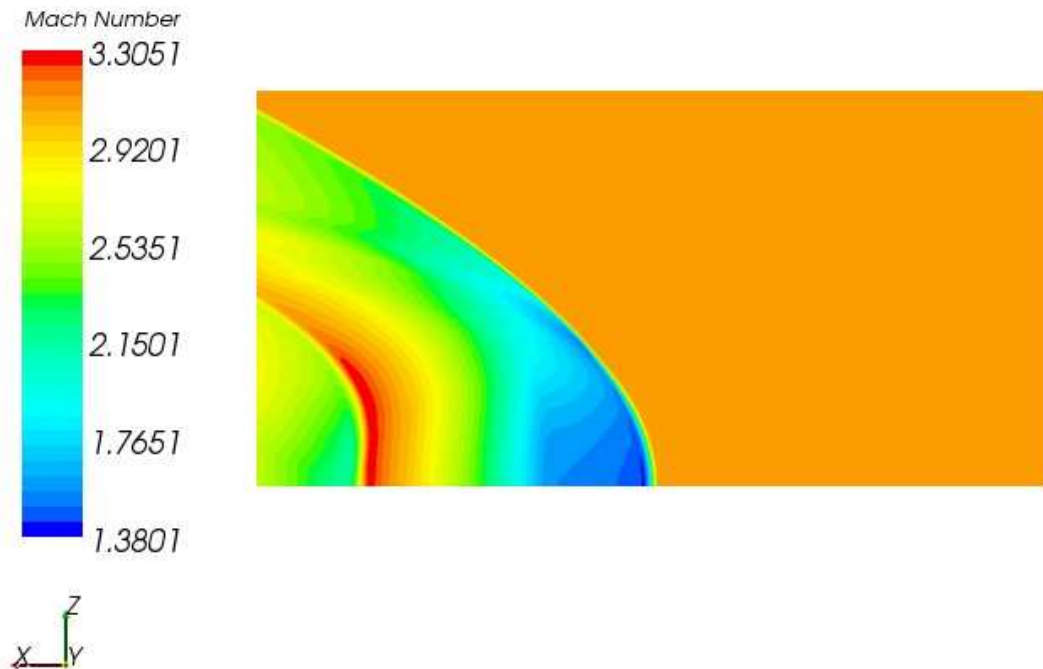


**Figure 31: A flooded plan view of Mach number plotted on the horizontal symmetry plane. This is for  $M_\infty = 3.1$ .**

Figure 31 shows a flooded plan plot of Mach number on the horizontal symmetry plane for the single transition case. As one can observe the incident shock wave is curved with supersonic flow behind the oblique shock wave.

All this is well illustrated in figure 32 below where a flooded plot of Mach number is plotted on the vertical symmetry plane.

As mentioned earlier figure 31 is a flooded plot of Mach number plotted on the vertical symmetry plane, whereby Starccm+ is used as the CFD solver.

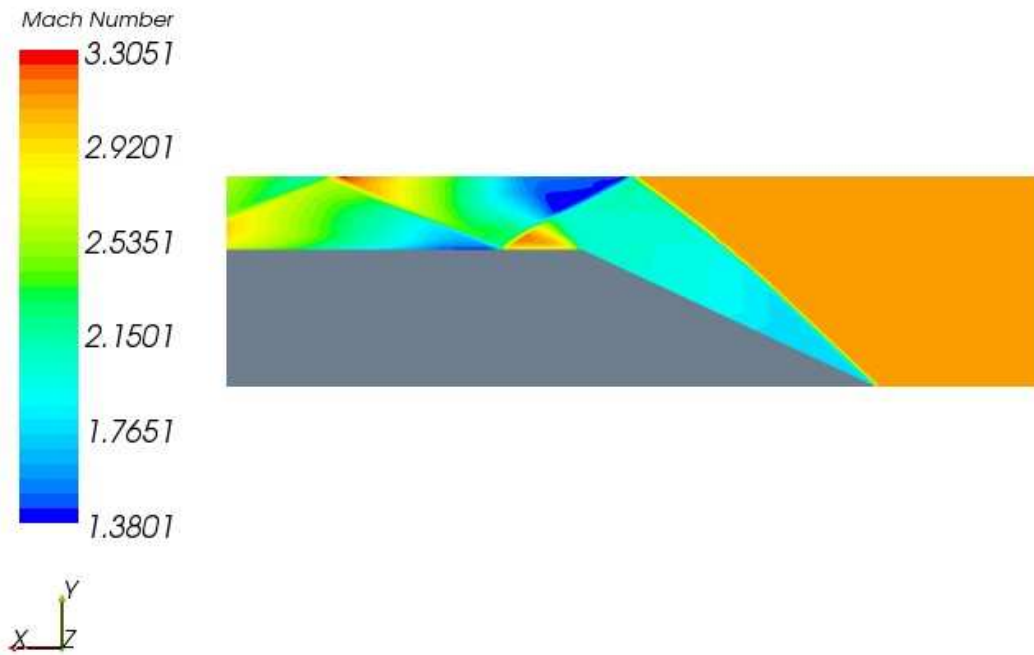


**Figure 32: A flooded plan view of Mach number plotted on the vertical symmetry plane. This is for  $M_\infty = 3.1$ .**



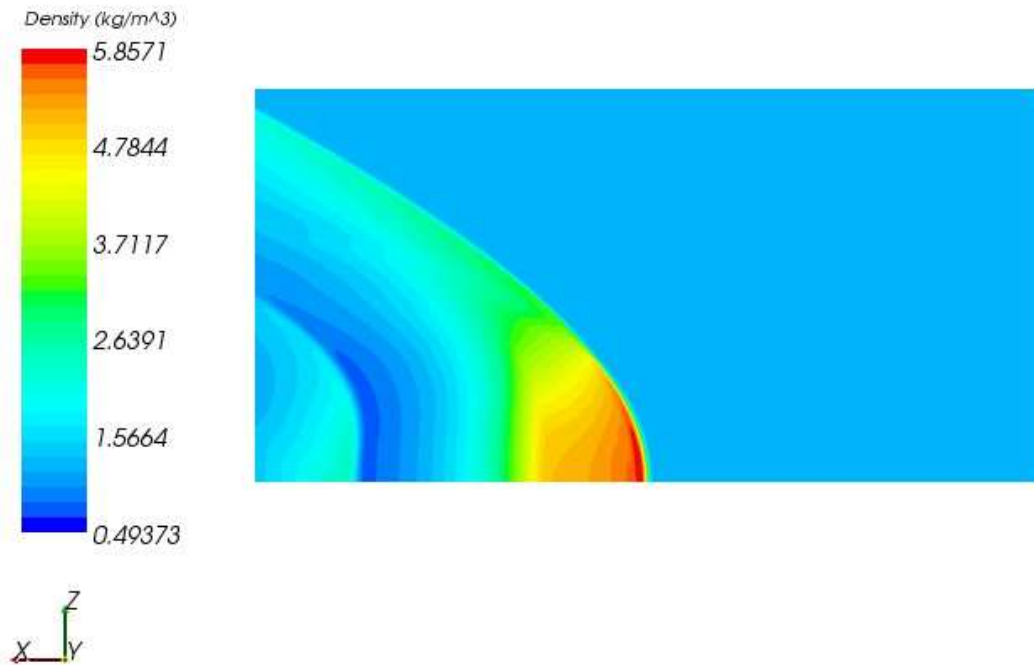


**Figure 33:** A flooded plan view of density plotted on the horizontal symmetry plane. This is for  $M_\infty = 3.1$ .

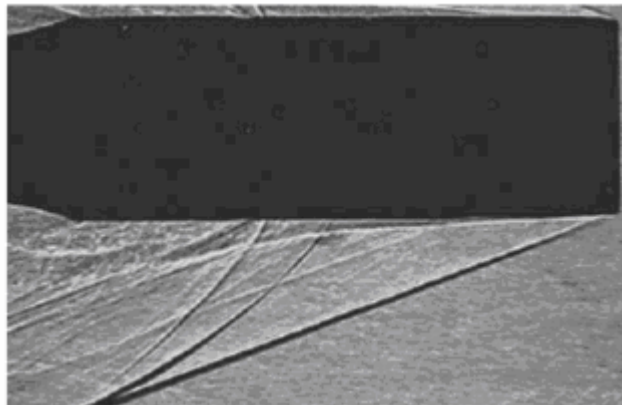


**Figure 34:** Orthogonal shadowgraph showing the single transition phenomenon. This picture is the same figure 8, but rotated by  $180^\circ$  for easy comparison with figure 29. Adapted from Brown and Skews (2004).

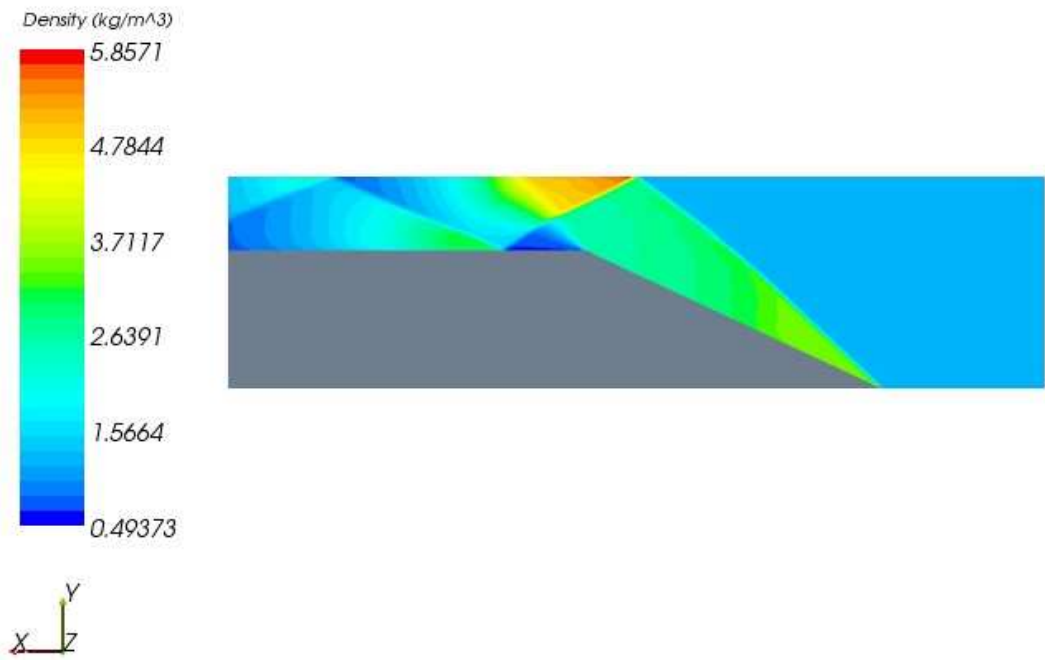


**Figure 35: A flooded plan view of density plotted on the vertical symmetry plane. This is for  $M_\infty = 3.1$ .**

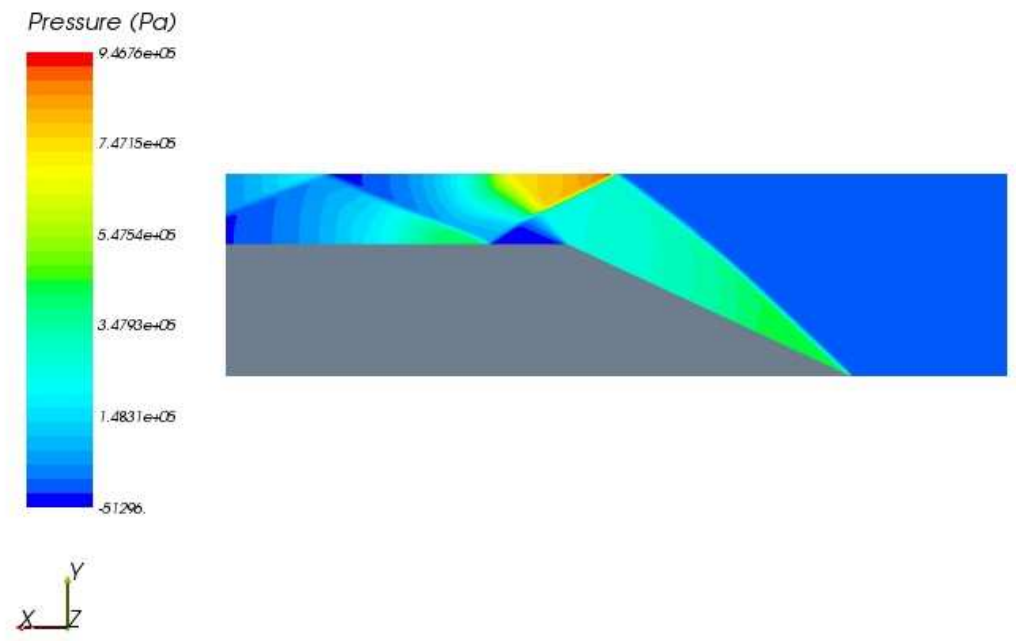


Figure 36: A flooded plan view of pressure plotted on the vertical symmetry plane. For  $M_\infty = 3.1$ .

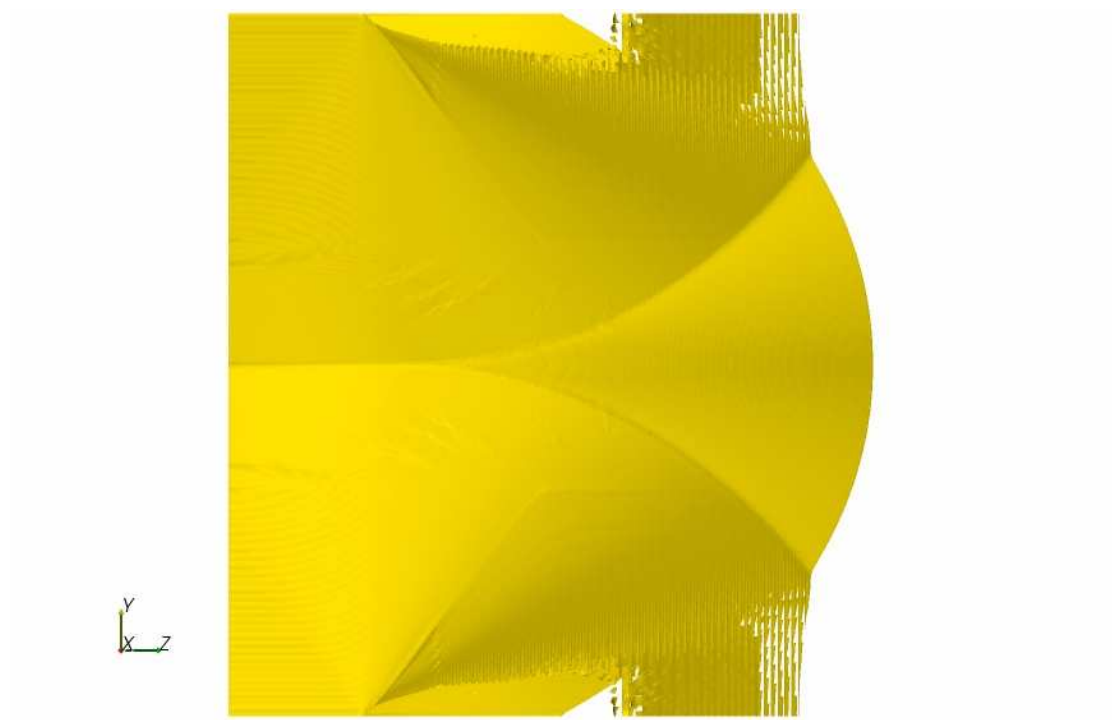


Figure 37: A front view of Mach=2.9 isosurface showing the right half of the single transition phenomenon with the vertical plane of symmetry to the left. This is for  $M_\infty = 3.1$ .



**Figure 38: A close-up of Figure 37.**

The shape of the transition is shown in figures 37 and 38. From both figures it can be seen that the transition is smooth and not sudden contrary to the experimental observation by Skews (2000).



**Figure 39: A front view of Mach=2.9 isosurface showing the lower half of the single transition phenomenon below the horizontal plane of symmetry. This is for  $M_\infty = 3.1$ .**

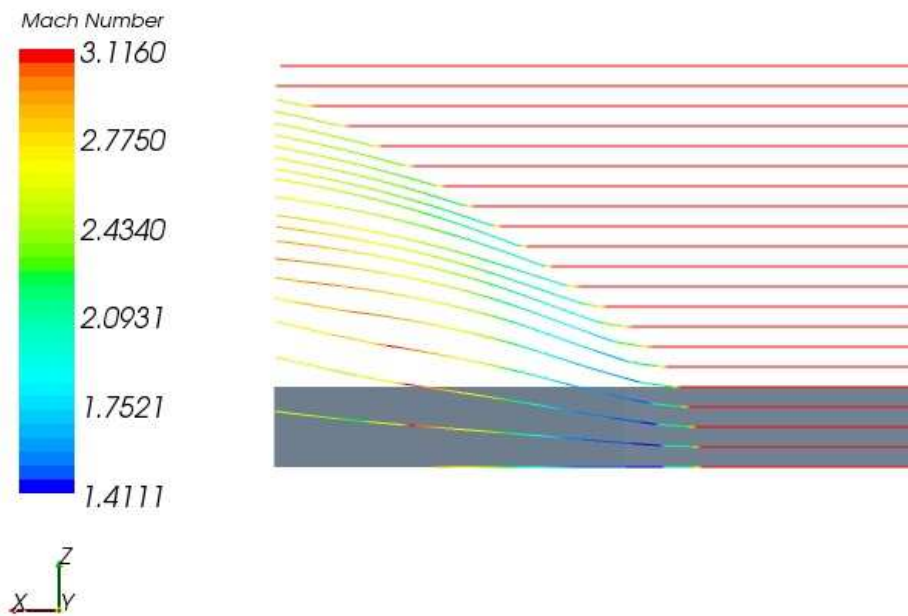


**Figure 40: A plan view showing streamlines paths being affected by going through shock waves. For  $M_\infty = 3.1$ .**

The effect that the shock waves have on the flow is easily illustrated with the use of streamlines as in figure 40. From the figure it is seen that with flow coming from the right, the flow is generally deflected towards the tunnel wall (being the top of the figure.) This effect is well pronounced in figure 41 showing how the flow moves towards the tunnel walls and away from the wedge surface.

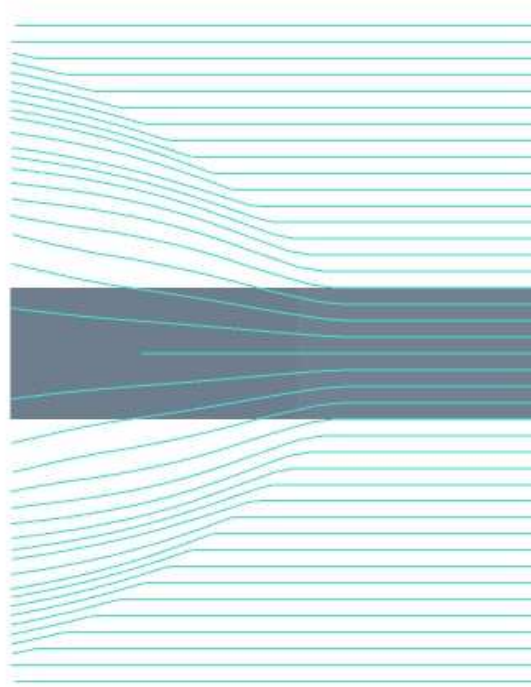


**Figure 41: A plan view showing streamlines paths being affected by going through shock waves, for both sides of the wedge. For  $M_\infty = 3.1$ .**

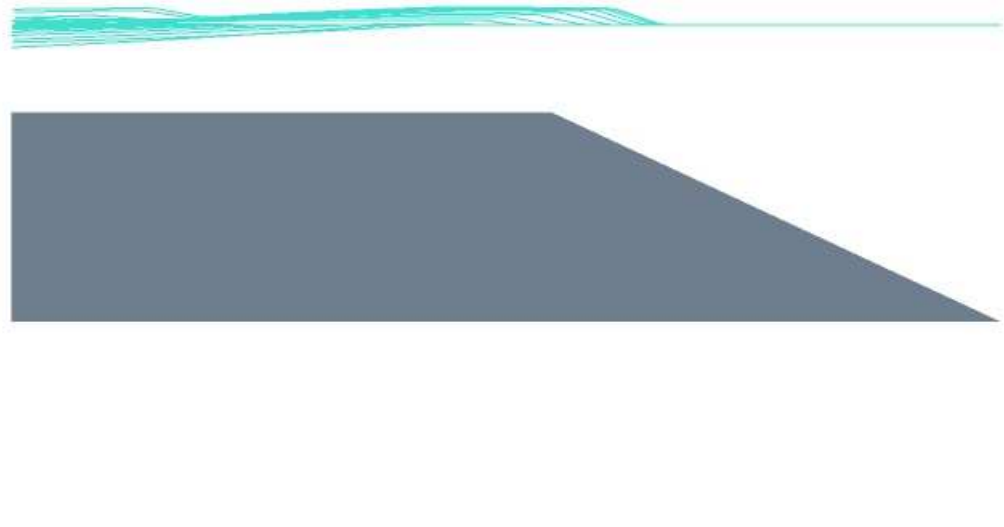


**Figure 42: A side view showing streamlines paths being affected by going through shock waves. For  $M_\infty = 3.1$ . streamlines released just below the horizontal plane of symmetry.**

From figure 42 one can see the effect that the incident shock wave has on the flow by observing that the streamlines are deflected upwards towards the horizontal symmetry plane. This is as expected as predicted by two-dimensional theory as to the trajectory of streamlines going through the shock wave. This effect is also seen in figure 43. Because figure 42 is viewed from the vertical symmetry plane, what is observed in the figure is the effect due to the regular reflection pattern. But the effect due to both the regular reflection and Mach reflection is observed in figure 43. The already observed upward deflection of the flow by the regular reflection pattern is to the right of the figure, whereas the observed zero change in height of the streamlines to the left of the figure is due to the Mach reflection pattern. Again this is as expected as predicted by two-dimensional theory. One can conclude that two-dimensional theory could be used in three-dimensional flow fields at different stations transverse to the stream wise direction, and the theory would be valid for that particular station.



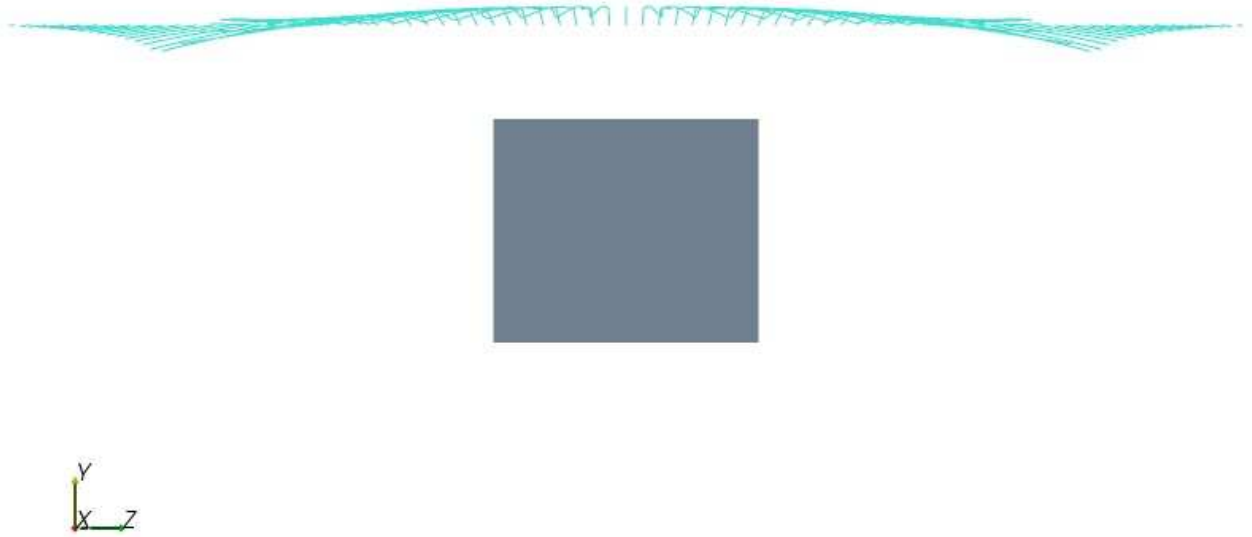


**Figure 43: A front view showing streamlines paths being affected by going through shock waves. For  $M_\infty = 3.1$ .**

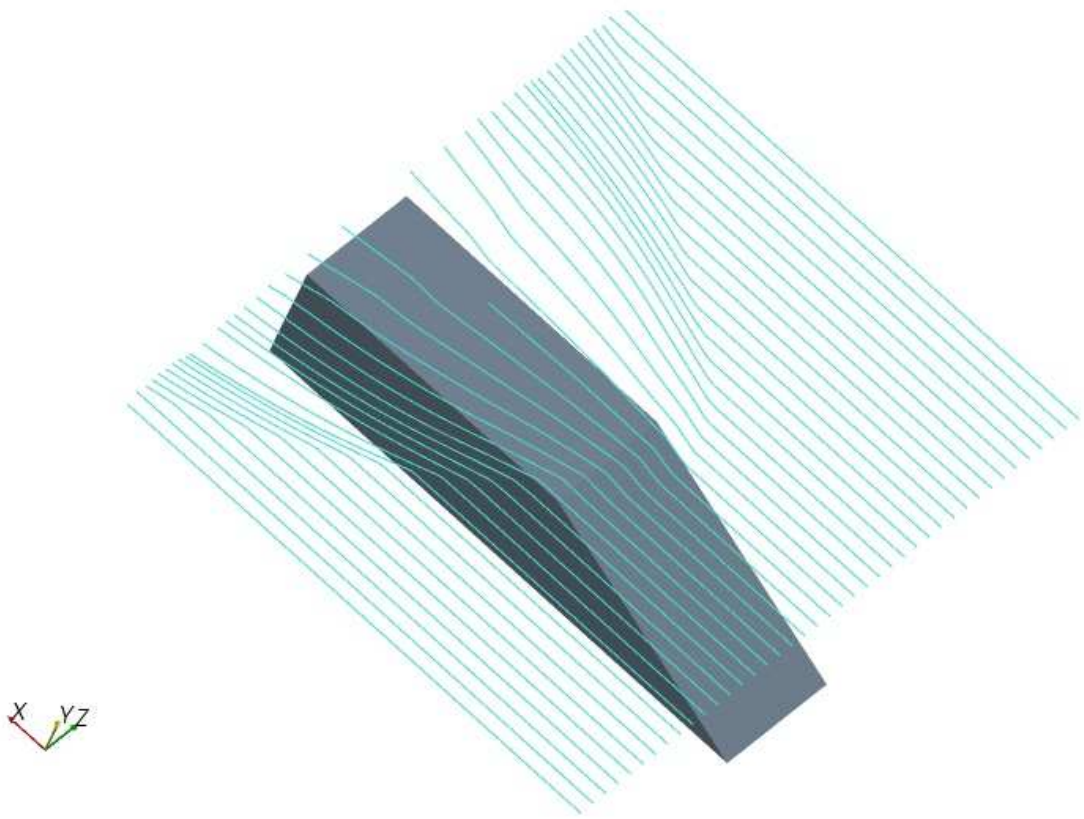


**Figure 44: An isometric view showing streamlines paths being affected by going through shock waves. For  $M_\infty = 3.1$ .**

## Conclusions

The sudden transition from regular reflection to Mach reflection observed experimentally by Skews (2000) could not be observed numerically when using two commercial CFD codes, a possible reason for this being the noisy wind tunnel used by Skews (2000). The reflection phenomenon observed experimentally by Ivanov et al. (1999) was replicated numerically using the two above mentioned commercial CFD codes for the same Mach number of 4 and a lower Mach numbers of 3.1 and 2.9, although for Mach 4 the simulation was unsteady.

## References

1. L. F. Henderson, A. Lozzi (1975), "Experiments on transition of Mach reflection", *J. Fluid Mech.*, Vol. 68, pp. 139-155.
2. M. S. Ivanov, G. P. Klemenkov, A. N. Kudryavstev, S. B. Nikiforov, A. A. Pavlov, A. M. Kharitonov, V. M. Fomin (1999), "Wind tunnel experiments on shock wave reflection transition and hysteresis", 22<sup>nd</sup> International symposium on Shock waves, Imperial College, London, UK, paper 1121.
3. B. W. Skews, J. A. Mohan, N. Menon (2004) Unexpected wave patterns in a non-circular supersonic duct inlet. 4<sup>th</sup> South African Conference on Computational and Applied Mechanics, SACAM 2004, Mist hills, Johannesburg, South Africa.
4. B. W. Skews (2000), "Three-dimensional effects in wind tunnel studies of shock wave reflection", *J. Fluid Mech.*, Vol. 407, pp. 85-104.
5. N. Sudani, M. Sato, T. Karasawa, A. Tate, J. Noda, M. Watanabe, Y. Mizobuchi, S. Hamamoto, "Effects of three-dimensionality and asymmetry on transition to Mach reflection", 22<sup>nd</sup> International symposium on Shock waves, Imperial College, London, UK, paper 1999.
6. A. Chpoun, E. Leclerc (1999), "Experimental investigation of the influence of downstream flow conditions on Mach stem height", *Shock Waves* 9, pp. 269-271.
7. A.N. Kudryavtsev, D.V. Khotyanovsky, M.S. Ivanov, A. Hadjadj, D. Vandromme (2002), "Numerical investigations of transition between regular and Mach reflections caused by free-stream disturbances", *Shock Waves* 12, pp. 157-165.
8. H. Horning (1986), "Regular and Mach reflection of shock waves", *Ann. Rev. Fluid Mech.* 18, pp. 33-58.
9. L. F. Henderson, K. Takayama, W. Y. Crutchfield & S. Itabashi (2001), "The persistence of regular reflection during strong shock diffraction over rigid ramps", *J. Fluid Mech.*, vol. 431, pp. 273-296.
10. G. Ben-Dor, O. Igra, T. Elperin (2001), *Handbook of Shock Waves*, vol. 2.

11. Y.A. Irving-Brown, B.W. Skews (2004), "Three-dimensional effects on regular reflection in steady supersonic flows", *Shock Waves* 13, pp. 339–349.

## Appendix A: Additional pictures for the double transition case.

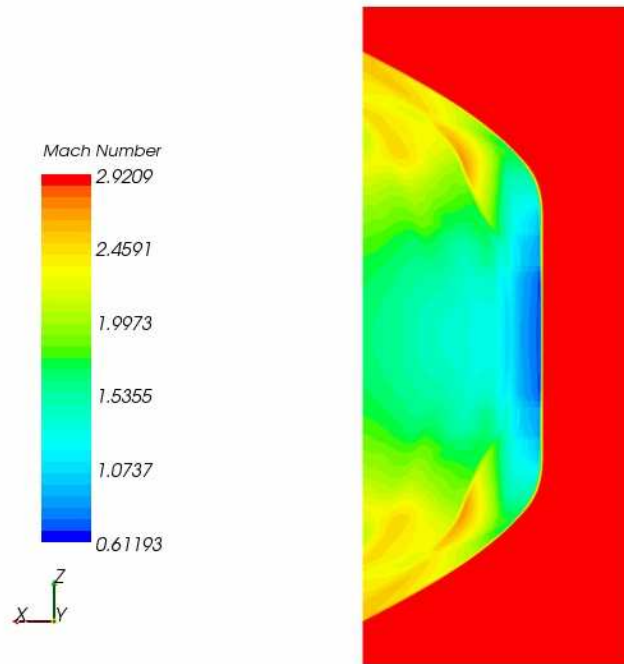


Figure 44: A flooded plan view of Mach number plotted on the horizontal symmetry plane. This is for  $M_\infty = 2.9$

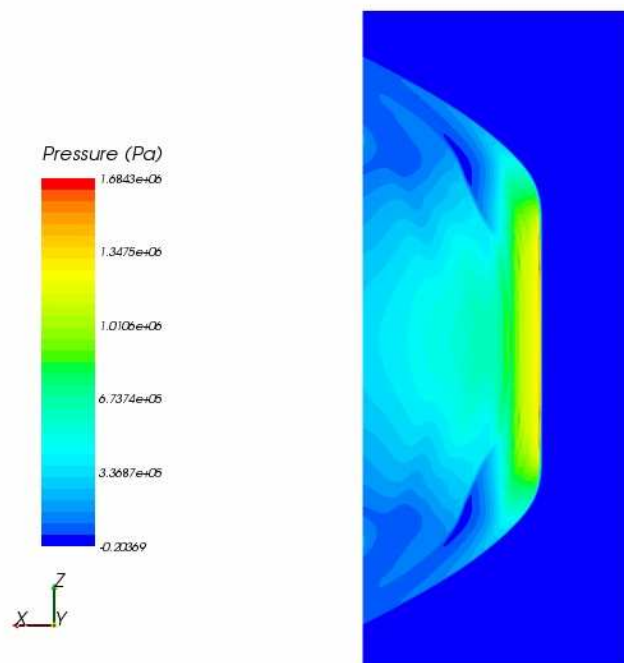
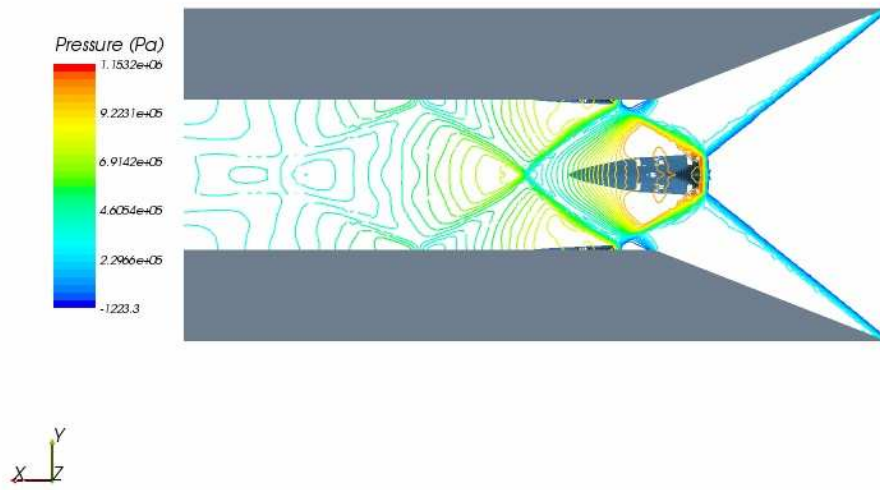


Figure 45: A flooded plan view of Pressure plotted on the horizontal symmetry plane. This is for  $M_\infty = 2.9$



**Figure 46:** A contoured side view of Pressure plotted on the vertical symmetry plane superimposed with the slip surface, showing the shape of the slip surface viewed from the side. This is for  $M_{\infty} = 3.1$

## Appendix B: Additional pictures for the single transition case.

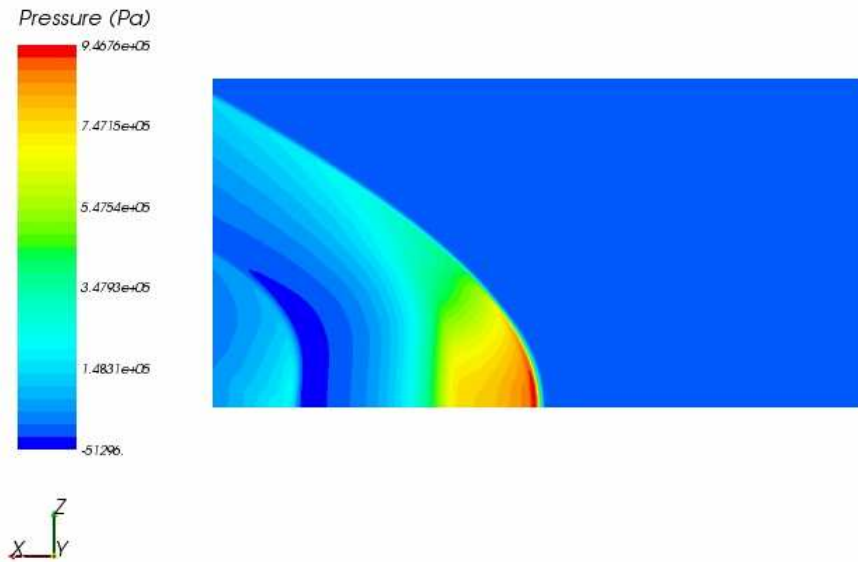
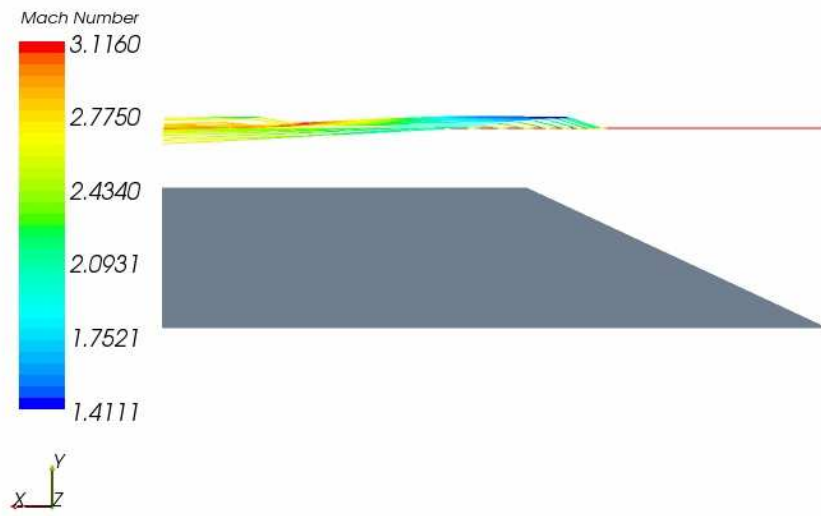
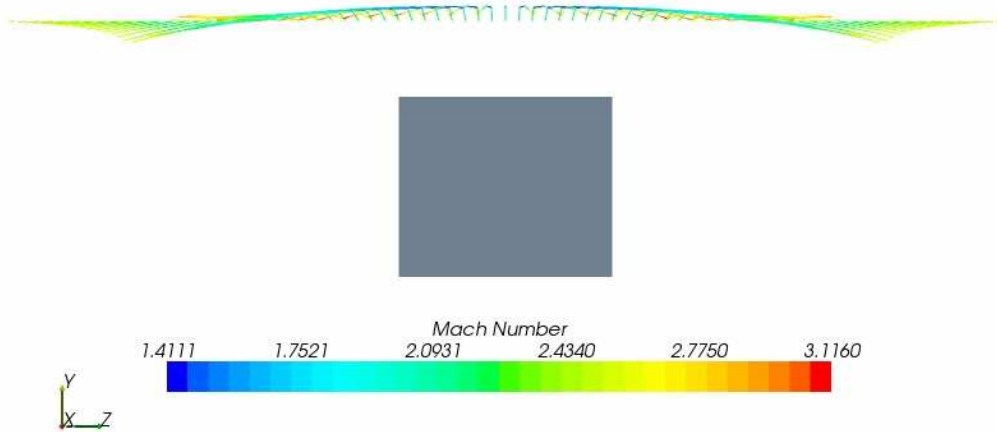


Figure 47: A flooded plan view of Pressure plotted on the horizontal symmetry plane.



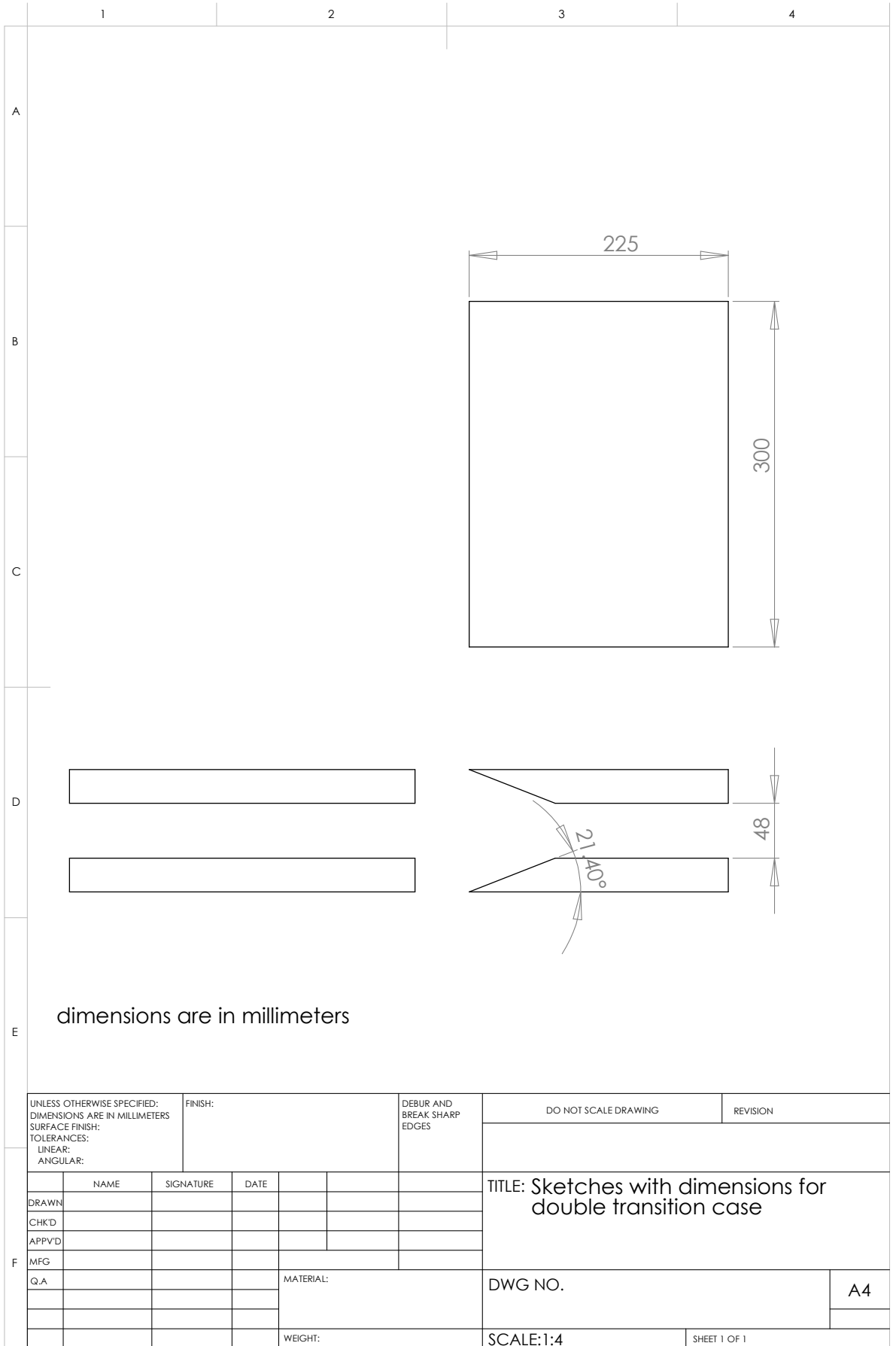


**Figure 48:** A side view showing streamlines (in colour) paths being affected by going through shock waves. For  $M_\infty = 3.1$ . Streamlines released just below the horizontal plane of symmetry.

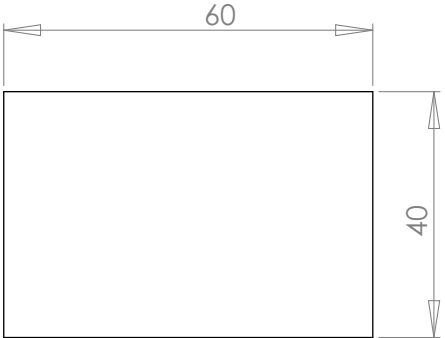
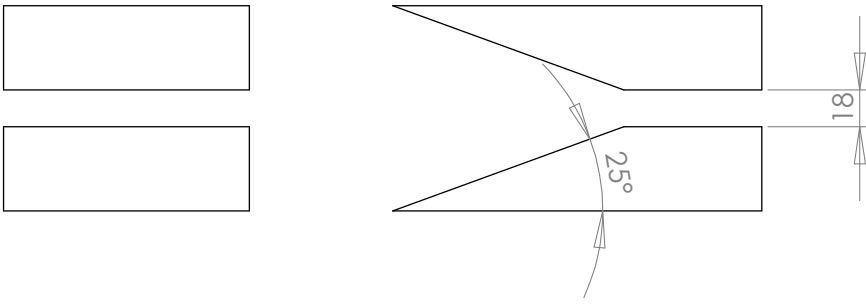


**Figure 49:** A front view showing streamlines paths (in colour) being affected by going through shock waves. For  $M_\infty = 3.1$ .

**Appendix C: Detailed dimensions of the wedge setup  
for each test case.**



UNLESS OTHERWISE SPECIFIED: DIMENSIONS ARE IN MILLIMETERS SURFACE FINISH: TOLERANCES: LINEAR: ANGULAR:		FINISH:		DEBUR AND BREAK SHARP EDGES		DO NOT SCALE DRAWING		REVISION	
DRAWN		SIGNATURE		DATE		TITLE: Sketches with dimensions for double transition case			
CHK'D									
APPVD									
MFG						DWG NO.		A4	
Q.A						MATERIAL:			
						WEIGHT:		SCALE: 1:4	
								SHEET 1 OF 1	

1	2	3	4				
A							
B							
C							
D							
E	<p>Dimensions are in millimeters</p>						
F	<table border="1" style="width: 100%; border-collapse: collapse;"> <tr> <td style="width: 30%; font-size: 8px;">UNLESS OTHERWISE SPECIFIED: DIMENSIONS ARE IN MILLIMETERS SURFACE FINISH: TOLERANCES: LINEAR: ANGULAR:</td> <td style="width: 30%; font-size: 8px;">FINISH:</td> <td style="width: 40%; font-size: 8px;">DEBUR AND BREAK SHARP EDGES</td> </tr> </table>		UNLESS OTHERWISE SPECIFIED: DIMENSIONS ARE IN MILLIMETERS SURFACE FINISH: TOLERANCES: LINEAR: ANGULAR:	FINISH:	DEBUR AND BREAK SHARP EDGES	DO NOT SCALE DRAWING	REVISION
UNLESS OTHERWISE SPECIFIED: DIMENSIONS ARE IN MILLIMETERS SURFACE FINISH: TOLERANCES: LINEAR: ANGULAR:	FINISH:	DEBUR AND BREAK SHARP EDGES					
	DRAWN	NAME	SIGNATURE	DATE	<p style="font-size: 12px; margin: 0;">TITLE: Sketches and dimensions for the Single transition case</p>		
	CHK'D						
	APPVD						
	MFG						
	Q.A				MATERIAL:	DWG NO.	A4
					WEIGHT:	SCALE:1:1	SHEET 1 OF 1

